Åbo Akademi University

Jasmina Obradovic

Engineering of novel cellulose-based biocomposites and biofoams

Engineering of novel cellulose-based biocomposites and biofoams

Jasmina Obradovic

Laboratory of Fibre and Cellulose Technology
Faculty of Science and Engineering
Åbo Akademi University
Åbo, Finland, 2017

Supervised by
Professor Pedro Edson Fardim
Laboratory of Fibre and Cellulose Technology
Faculty of Science and Engineering
Åbo Akademi University
Finland
and
Department of Chemical Engineering
Faculty of Engineering Science
KU Leuven
Belgium

Co-supervised by
Academic Lecturer Jan Gustafsson
Laboratory of Fibre and Cellulose Technology
Faculty of Science and Engineering
Åbo Akademi University
Finland

Reviewers
Dr., FiDiPro Tatiana Budtova
Polymer and Composite Department
Centre de Mise en Forme des Materiaux CEMEF
Mines ParisTech
France

Professor Johannes Ganster
Biopolymers Division
Fraunhofer- Institut fur Angewandte Polymerforschung IAP
Germany

Opponent
Dr., FiDiPro Tatiana Budtova
Polymer and Composite Department
Centre de Mise en Forme des Materiaux CEMEF
Mines ParisTech
France

ISBN 978-952-12-3635-8 (printed version)
ISBN 978-952-12-3636-5 (digital version)
Painosalama Oy-Turku, Finland 2017

Abstract

Jasmina Obradovic
Engineering of novel cellulose-based biocomposites and biofoams

Doctoral Thesis
Åbo Akademi University, Fibre and Cellulose Department, Turku 2017, Finland.

Keywords: N,N-dimethylacetamide, acrylated epoxidized soybean oil, cellulose, composite, dissolution, foam, forging, lithium chloride, mechanical properties, moulding, porosity, pressure, pretreatment, regeneration, shellac, softwood dissolving pulp, solvent system, swelling

---

Biomass is a renewable feedstock for producing fine chemicals, polymers, energy, and a variety of commodities. Transformation of biomass into diverse valuable products is the key concept of a bioeconomy. Chemical and mechanical conversion of biomass, which reduces the use of toxic chemicals is one of the important approaches to improve the profitability of bioeconomy. Utilization of green materials under environmentally-friendly conditions, was the main goal of this research.

Wood fibres were converted into cellulose-based 3D objects through swelling of cellulose fibres in an N,N-dimethylacetamide and lithium chloride solvent system followed by a moulding step. Swollen cellulose pulp in the form of gel was solidified with two different anti-solvents. The choice of solidification solvent had a great influence on the structure and mechanical properties of the final cellulose material which was studied with x-ray diffraction and nanoindentation technique. The mechanical properties and optical properties of solid swollen cellulose fibres can be significantly increased with forging technique.

Bio-based composite materials composed of a mixture of shellac resin and cellulose fibres were developed. The influence of the reinforcement content and the concentration of additives on the mechanical performance and processing were investigated. A high amount of cellulose and low concentrations of ethanol and polyethylene glycol produced bio-based composites with high stress resistance, while a low amount of cellulose and high concentration of additives provided specimens with an increased elasticity.

Acrylated epoxidized soybean oil and variable amounts of wood fibres were used in a production of bio-based foam. The developed macroporous polymers were characterized by several techniques, including porosity measurements, nanoindentation testing, scanning electron microscopy and thermogravimetric analysis. It was found that the introduction of pulp fibres during the foaming process was necessary to create the polymer foams. Cellulose fibres behaved as

foam stabilizer while simultaneously acting as reinforcing agent in the polymer foam.

Sammanfattning

Jasmina Obradovic
Processering av nya cellulosabaserade biokompositer och bioskum

Doktorsavhandling
Åbo Akademi, Laboratoriet för Fiber- and Cellulosateknologi, Åbo, 2017.

Nyckelord: N,N-dimetylacetamid, akrylerad epoxiderad sojabönsolja, cellulosa, komposit, upplösning, skum, formning, litium klorid, mekaniska egenskaper, gjutning, porositet, tryck, förbehandling, regenerering, schellack, barrvedsdissolvingmassa, lösningssystem, svällning

---

Biomassa är ett förnybart råmaterial för att tillverka finkemikalier, polymerer, energi och en mängd handelsvaror. Omvandling av biomassa till diverse värdefulla produkter är nyckelkonceptet för ett bioraffinaderi. Kemisk och mekanisk konvertering av biomassa, vilket minskar användningen av giftiga kemikalier, är ett av de viktigaste tillvägagångssätten för att förbättra bioekonomins lönsamhet. Användningen av gröna material under miljövänliga förhållanden var huvudmålet för denna forskning.

Vedfibrer konverterades till cellulosabaserade 3D-objekt genom svällning av cellulosafibrer i ett lösningssystem av N,N-dimetylacetamid och litiumklorid, med ett därpå följande formningssteg. Uppsvälld cellulosamassa i gelform solidifierades med två olika antilösningsmedel. Valet av solidifieringslösningsmedel hade en stor inverkan på strukturen och de mekaniska egenskaperna av det slutliga cellulosamaterialet, vilket undersöktes med XRD- och nanoindeteringsmetoder. De mekaniska och optiska egenskaperna av fasta svullna cellulosafibrer kan väsentligt ökas genom formningtekniker.

Biobaserade kompositmaterial bestående av en blandning av schellackharts och cellulosafibrer utvecklades. Inverkan av armeringsmaterialhalten och koncentrationen av tillsatsmedel på den mekaniska prestandan och processeringen undersöktes. En hög halt av cellulosa och låga koncentrationer av etanol och polyetylenglykol producerade bio-baserade kompositer med hög spänningstålighet, medan en låg halt av cellulosa och en hög koncentration av tillsatsmedel ledde till prov med en ökad elasticitet.

Akrylerad epoxiderad sojabönsolja och en varierande mängd av vedfibrer användes för att tillverka bio-baserat skum. De utvecklade makroporösa materialen karakteriserades med flera tekniker, bland annat porositetsmätningar, nanoindentering, SEM och termogravimetrisk analys. Det upptäcktes att införandet av massafibrer under skumtillverkningsprocessen var nödvändig för att skapa polymerskummen. Cellulosafibrerna fungerade som

skumstabilisatorer samtidigt som de verkade som armeringsmedel i polymerskummet.

Table of contents

List of Figures

List of Tables

List of abbreviations and symbols

Abbreviation Symbol	*Explanation*
^{13}C NMR	carbon-13 nuclear magnetic resonance
3 D	three dimensional
AESO	acrylated epoxidized soybean oil
AGU	D-anhydroglucopyranose repeat unit
ATR-IR	attenuated total reflection infrared
Cell_2PDW	swollen softwood pulp solidificated with solvent composed of 2-propanol and deionized water
Cell_DW	swollen softwood pulp solidificated with distilled water
CO_2	carbon dioxide
DMAc	N,N-dimethylacetamide
DP	degree of polymerization
E	Young's modulus/ elastic modulus
EtOH	ethanol
FE-SEM	field emission scanning electron microscopy
FTIR	Fourier transform infrared spectrometry
H	hardness
ICP-MS	inductively coupled plasma mass spectrometry
LC	low consistency
LiCl	lithium chloride
NI	nanoindentation
PEG	polyethylene glycol
SWDP	softwood dissolving pulp
TGA	thermogravimetric analysis
UV-Vis	ultraviolet visible spectrometry
XRD	x-ray diffraction analyses
ε	porosity of foam using Ar pycnometer

Preface

The research work in this thesis was carried out in the Laboratory of Fibre and Cellulose Technology at Åbo Akademi University during 2011-2017. At the beginning, I was appointed as a researcher in a FuBio project funded by the Finnish Funding Agency for Innovation (Tekes). In 2014, I was granted a position in the Graduate School of Chemical Engineering (GSCE). The results are published in peer-reviewed scientific journals and are referred in the text as Paper I-IV.

List of publications and authors contribution

I. Obradovic, J., Wondraczek, H., Fardim, P., Lassila, L., and Navard, P. (2014). *Preparation of three-dimensional cellulose objects previously swollen in DMAc/LiCl solvent system*, Cellulose 21(6), 4029-4038.

II. Obradovic, J., Fardim, P., Lassila, L., and Navard, P., Kronlund, D. (2015). *High-pressure treatment of DMAc/LiCl swollen softwood pulp*, Bioresources 10(2), 2130-2142.

III. Obradovic, J., Petibon, F., Fardim, P. (2017). *Preparation and characterisation of cellulose-shellac biocomposite*, Bioresources 12(1), 1943-1959.

IV. Obradovic, J., Voultainen, M., Virtanen, P., Lassila, L., Fardim, P. (2017). *Cellulose fibre reinforced biofoam for structural applications*, Materials 10(6), 619.

Author's contribution: All parts, including writing the manuscripts, excluding analysis performed with ICP-MS, XRD, Ar-pycnometry and preparation of the cellulose-shellac composite specimens.

List of supporting proceedings and presentations

1. Obradovic J., Fardim P., *Preparation of mouldable cellulose materials*. 1st International Conference on Natural Fibres, Proceedings, pp. 395-396, 2013, Guimarães, Portugal.

2. Obradovic J., Fardim P., *Mouldable cellulose materials*. COST Action FP1205 - Training school, Poster, 2014, Valencia, Spain.

3. Obradovic J., Fardim P., Narewska J., *Biocomposite based on pulp fibres and acrylated epoxidized soybean oil*. 23rd Annual International Conference on Composites and Nano Engineering, Proceedings, pp. 591-592, 2015, Chengdu, China.

4. Obradovic J., Wodraczek H., Lassila L., Navard P., Fardim P., *Mouldable cellulose-based materials*. I&S Workshop on insights and strategies towards a bio-based economy, Proceedings, pp. 13-14, 2016, Montevideo, Uruguay.

5. Obradovic J., Fardim P., *Cellulose-shellac biocomposite for packaging application*. 7th Nordic Wood Biorefinery Conference, Proceedings, pp. 234-235, 2017, Stockholm, Sweden.

1. Introduction

Biomass, including wood, agricultural crops and grasses, is the largest and most important renewable option at present and can be used to produce different forms of materials and energy. As a result, biomass resources are capable of providing part of the commodities required in a modern society, both locally and in most parts of the world. Renewability and versatility are, among many other aspects, important advantages of biomass as a resource.

Wood and wood-based materials have been used by humans since the very beginning due to their availability and versatility. Wood biomass today is mostly used for pulp and paper production. The pulping process has been improved throughout the years so that the cellulose is utilized efficiently, while the rest is burned to obtain energy. Cellulose, hemicellulose and lignin are the three main components of wood. Cellulose is a natural polymer found in large amounts in nearly all plants, and it is considered the most valuable fraction of biomass. Paper, cardboard and textiles are major products from cellulose fibres. Cellulose can be transformed in many different products through either dissolving and regenerating or derivatizing processes.

Currently there are a few approaches to produce regenerated cellulose, such as Cupro, Viscose and Lyocell [1]. Processes involving ionic liquids [2] can also dissolve cellulose, but high cost and solvent recovery problems hinder their further application. Fundamental understanding of the cellulose dissolution chemistry is of great interest for chemical engineers. If an effective and economical cellulose dissolution method can be developed, a new platform for producing cellulosic materials will be created, providing new opportunities for using cellulose as a sustainable engineering polymer.

The main aim of this research was to prepare novel functional materials from pulp fibres. The goal was to prepare cellulose-based material with the usage of less toxic solvent and lower power input. In that fashion, green material can be produced where cellulose fibers are swollen and regenerated. Such an approach was later followed for the creation of both bio-based composites and bio-based foams.

1.1. Wood and pulp fibres

1.1.1. Structure of wood

Wood biomass has always held a significant place in the human evolution. Fruits, seeds, flowers, leaves and other parts of wood have been utilized as food, clothing or medicine, while wood stem served as an energy source, building material, furnishes, tools and weapons. Even though the manner of utilization has shifted over time, the place of wood in the economy has remained very important.

Wood represents one of the most important renewable natural resources. The annual growth is sufficient to satisfy many needs. Humans utilize 6 billion

metric tons of biomass annually. Food consumption accounts for 62% of use, while wood consumption for energy, paper, furniture, and construction uses 33%. The remaining 5% is consumed for other non-food purposes, including energy, chemicals, clothing, plastics, and other man-made fibres [3]. Approximately one third of the earth's land area is now forested. The remaining area involves deserts, grasslands, and arctic tundra. However, some forest lands are converted to agricultural fields due to fertile soil or favourable topography.

Wood is a heterogeneous material, and it is formed during the growth of plants. A plant is a tissue of very different kinds of cells performing functions, namely water conduction, metabolism, and mechanical support. These cells remain in mature wood as a network of cell walls [4].

A tree is commonly considered to have three major parts, the stem, the crown and the roots. The leaf is the main factory of wood. It is an organ in which the food is manufactured by photosynthesis. The stem of the tree is a raw material mostly used in industry. The root system is extensive as the crown, and it anchors the tree to the ground, absorbs nutrients from the soil, transports nutrients to the stem, and stores reserve food.

The tree species can be divided into two different groups of plants that have very different evolutionary strategies. Both species rely on their leaves to convert water, carbon dioxide, and nutrients into energy that they can use to grow and reproduce. Most conifers (gymnosperms) keep their leaves year round, while many deciduous trees (angiosperms) shed their leaves in the fall and grow new ones in the spring.

1.1.2. Chemical composition of wood

The chemical composition of wood is complex. The wood material is made up of many structural and non-structural components. The greater part of a tree is composed of substances with high molecular weight. The separation and isolation of these polymers without modification is a difficult and challenging task.

The major part in wood represents polysaccharides. They include cellulose, hemicellulose, starch, and pectic substances (Figure 1.1). The next group of chemicals is aromatic materials characterized by the presence of phenolic hydroxyl groups. Representative of aromatic substances is lignin, a material of high molecular weight, insoluble in common solvents. Terpen and terpenoid present in softwood include volatile constituents and the resin acids. Aliphatic acids, alcohol, proteins and inorganic materials also occur in wood in small amounts. The element content of wood is about 50% carbon, 6% hydrogen, 44% oxygen, and 0.05–0.4% nitrogen.

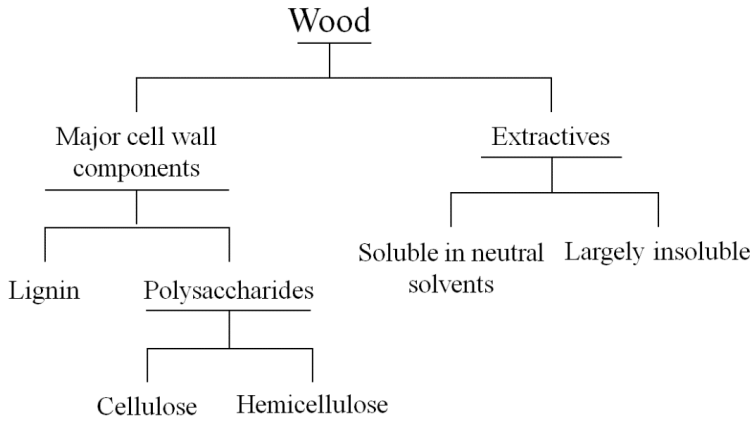

Figure 1.1 Composition of wood.

The plant cell wall in wood tissue has a multicomposite structure, consisting of several layers formed at different periods during cell differentiation. Wood cell walls consist mainly of three biopolymers: cellulose, hemicellulose, and lignin. It is made of a network of cellulose microfibrils embedded in a matrix of lignin and hemicellulose. Between adjacent cells, a middle lamella layer attached to the primary cell wall ensures the adhesion of a cell to its neighbour (Figure 1.2).

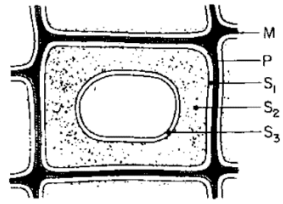

Figure 1.2 Cross-section of wood fibre cell. M-middle lamella, P-primary wall, S1- outer layer of the secondary wall, S2- secondary wall, S3- inner layer of the secondary wall [5].

Primary cell walls are synthesized during growth and typically are relatively thin, pliant, and highly hydrated structures. Primary walls are comprised of 15–40% cellulose, 30–50% pectic polysaccharides, and 20–30% xyloglucans and lesser amounts of arabinoxylans and structural proteins [6]. The secondary cell walls provide strength and rigidity in plant tissues that have ceased growing. Secondary cell wall consists of three different sublayers (S1, S2, and S3). The cellulose microfibril orientation and chemical composition varies between the sublayers (Figure 1.3). The S2 layer is the thickest (75%–85% of the total thickness of the cell wall) and most important for mechanical stability [7].

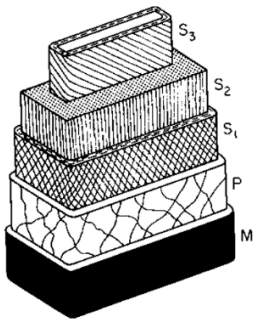

Figure 1.3 Cross-section of wood fibre cell. M-middle lamella, P-primary wall, S1- outer layer of the secondary wall, S2- secondary wall, S3- inner layer of the secondary wall [5].

Cellulose is a linear homopolymer of β-(1,4)-linked D-anhydroglucopyranose monomeric repeat units (AGU). Every second glucose unit is sterically rotated by approximately 180 º with respect to its neighbours (Figure 1.4). Each monomeric repeat unit possesses three hydroxyl groups, in position C-2, C-3, and C-6 of the pyranose unit. The nonreducing end has an additional OH-group in position C-4, and reducing end features carbonyl functionality. The size of a cellulose molecule is expressed as the degree of polymerization (DP), which is the number of AGUs per chain. In natural size, cellulose is thought to have 14,000 glucose units. Commercially available cellulose has a range of DP from 100 to 12,000 [8].

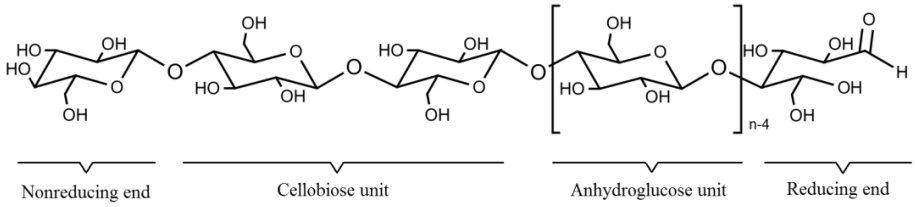

Figure 1.4 Chemical structure of cellulose molecule indicating two different repeat units and end groups.

Hemicelluloses represent a class of noncellulosic polysaccharides that is associated with cellulose in plant cell walls [9]. The term hemicellulose was first used by Schulze in 1887 in the belief that hemicelluloses were perhaps components that were on the way of becoming cellulose. It has long been recognized that the term is misleading, and that polyoses or heteropolysaccharides are better descriptors [10]. Heteropolysaccharides are classified into five primary classes: xylans, glucomannans, arabinans, galactans, and glucans. With few exceptions, these polysaccharides consist of linear homo-

or copolymers with variable degrees of branching and with occasional replacement of hydroxyl groups by *O*-acetyl groups. The most prominent group of heteropolysaccharides in hardwoods and annual plants are the xylans.

Native lignin in plants is a three-dimensional, cross-linked, phenolic heteropolymer with an amorphous character. It has much lower hydrophilicity than cellulose and hemicellulose. Lignin is the term for a large group of aromatic polymers resulting from the oxidative combinatorial coupling of 4-hydroxyphenylpropanoids. The main building blocks of lignin are the hydroxycinnamyl alcohols, coniferyl alcohol and sinapyl alcohol, with typically minor amounts of *p*-coumaryl alcohol [11].

1.1.3. Pulping process

Wood is converted to pulp for the production of paper, paper board, regenerated cellulose and cellulose derivatives. Pulping is the process of fibre separation (Figure 1.5). Separation of wood fibre can be purely mechanical, chemical or a combination of mechanical and chemical treatment. The choice of process depends on the requirements for purity, strength, and colour of the resulting pulp.

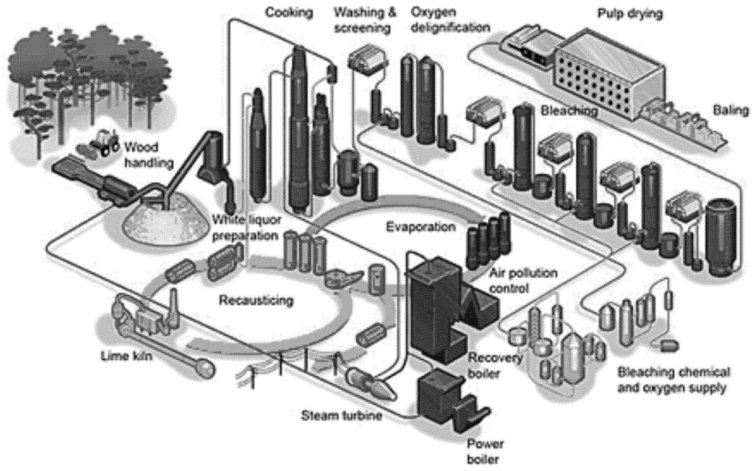

Figure 1.5 Image of a pulp production (Valmet).

The three-stage soda process, patented by Watt and Burgess in 1853 [12], was the first commercial pulping process. They produced pulp by boiling wood in caustic alkali at elevated pressure. Meanwhile, the mechanical pulping process was developed in Germany with a groundwood machine designed by Keller in 1940. Tilghman invented the sulfite process in 1866. He cooked wood chips in an acid solution of calcium bisulfite and sulfur dioxide [13]. The sulfite process was applied commercially 15 years later in Germany and Sweden. The sulfite

process was replaced by the kraft process discovered by German chemist Dahl. This method used additional sodium sulfate to produce strong pulps [14].

Chemical pulping including sulfate (kraft), soda, and sulfite are processes that accomplished delignification by chemical treatment. Digested chips are reduced to pulp upon blowing from the digester, and no other mechanical assistance is required. In semichemical pulping there is a necessity to apply mild mechanical treatment in the form of milling. The lignin is partially modified and a part is removed. Chemimechanical pulping combines chemical and mechanical action. The moderate chemically treated chips require extensive milling or grinding. The lignin is slightly modified and a small amount is removed. Mechanical pulping is accomplished by the grinding of bolts of wood with a grindstone or by the disk milling of chipped wood. Lignin modification and removal is negligible [15].

The chemical and physical properties of wood pulps vary with the wood species and the pulping process used. In the production of a dissolving pulp, the high purity and controlled distribution of the molecular weights is required. In the case of paper pulps, the physical properties are of main importance where the strength and bonding characteristics determine the quality of paper. Pulp properties are largely dependent on the morphology, structure and composition of fibres, and the structure and distribution of chemicals in the cell wall. Nevertheless, pulp characteristics are greatly influenced by the degree of delignification.

1.2. Cellulose fibres, solvent systems and compression methods

The first attempts to dissolve wood fibres or cellulose containing material were described about 150 years ago [16]. Since then a variety of cellulose solvents have been developed or were discovered by coincidence. Looking at the history of cellulose solvents, the first man-made fibre, silk, was obtained with a soluble cellulose nitrate by Chardonnet. The first man-made plastics, Celluloid and Parkesine, were prepared via the same modification reaction [17]. Historically, the next dissolution method for cellulose which involves partial derivatization was the viscose process. In 1891, the British chemists discovered that cotton or wood could be dissolved as cellulose xanthate followed by alkali and carbon disulphide treatment. The yellow solution could be coagulated in an ammonium sulphate bath and converted back to pure cellulose using dilute sulphuric acid.

Turbak [18] divided cellulose solvents into four main categories based on the possible interactions of cellulose with solvents. Philipp [19] modified this system dividing cellulose solvents into derivatizing, non-derivatizing, aqueous and non-aqueous solvents. Furthermore, this classification was combined with the number of components in the solvent system [20]. Alternatively, solvents can be grouped into certain modes of interaction with cellulose according to the morphological changes of the polymer determined by microscopy [21]. Generally, there are two big categories of cellulose solvents, non-derivatizing and derivatizing ones. The non-derivatizing solvents may be further subdivided

into metal-complex cellulose solvents (copper ethylenediamine (cuen) and cadmium oxide in ethylenediamine (cadoxen)), salt-free solvents (N-methylmorpholine-N-oxide monohydrate (NMMO)), salt containing solvents (DMAc/LiCl and $LiClO_4x3H_2O$), and ionic liquids.

Derivatizing solvents, or precisely derivatizing agents change the cellulose so that it becomes soluble, and solvents interact chemically with a cellulose on a molecular level. A well-known method of cellulose dissolution is previous chemical modification of the macromolecule. The main objective of this procedure is to functionalize the hydroxyl groups and to disrupt the intra- and intermolecular hydrogen bonding but with minimal chain degradation. Functionalization reactions of cellulose include nitration [22], xanthation [23], esterification [24], and etherification [25]. The solubility of the derivatized cellulose depends on the type and degree of derivatization. Most of the derivatives are soluble in common polar organic solvents like DMF, DMSO, and dioxane [26].

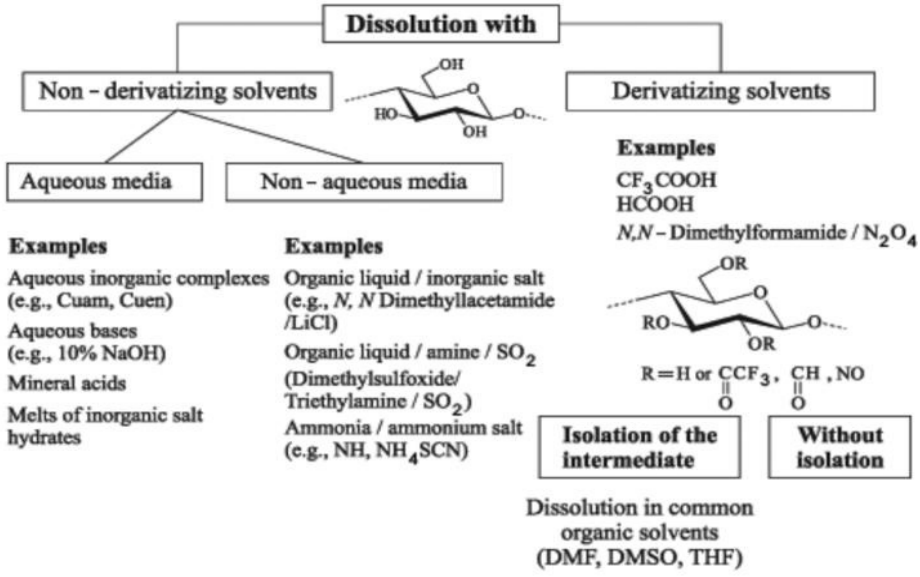

Figure 1.6 Classification of cellulose solvents [28].

Cellulose is neither meltable nor soluble in usual solvents including water and typical organic solvents. The huge difficulty in the dissolution process can be attributed to the complexity of such a biopolymeric network, the partial crystalline structure and the extended non-covalent interactions among molecules, making the chemical processing rather difficult. In Figure 1.6 the classification of the common cellulose solvents is represented.

A completely new type of solvent, capable of providing clear solutions of the polymer without chemical modification, was discovered by Graenacher [27]. He demonstrated that low melting organic salts can be applied as non-

aqueous, non-derivatizing cellulose solvents. In 2002, studies were published on the use of comparable salts with a melting point below 100ºC, known today as ionic liquids, as cellulose solvent. It was shown that the most promising ionic liquid for the modification of cellulose are 1-alkyl-3-methylimidazolium salts. According to literature ionic liquids with ammonium cations, pyridinium cations, and imidazolium cations are able to dissolve cellulose. Only organic salts with asymmetric cations give melts, which can interact with the cellulose backbone. Cellulose can be regenerated from solution in ionic liquids by precipitation with a variety of non-solvents including water, alcohol, and acetone.

1.2.1. Cellulose fibre and DMAc/LiCl solvent system

The first Li salt containing solvents was N,N-dimethylacetamide (DMAc)/LiCl, discovered in 1979 by McCormick [29]. The system N,N-dimethylacetamide (DMA)/LiCl shows an enormous potential for the analysis of cellulose and for the preparation of a wide variety of derivatives.

This solvent system is an important tool in analysis due to the fact that the solvent is colourless and dissolution succeeds with negligible degradation even in case of high molecular weight cellulose. Thus, it was possible to investigate the dissolved cellulose by means of size exclusion chromatography [30], ^{13}C-NMR spectroscopy [31] electrospray mass spectroscopy [32], and light scattering techniques [33]. The mechanism of cellulose dissolution in this solvent is still a topic of active research [34].

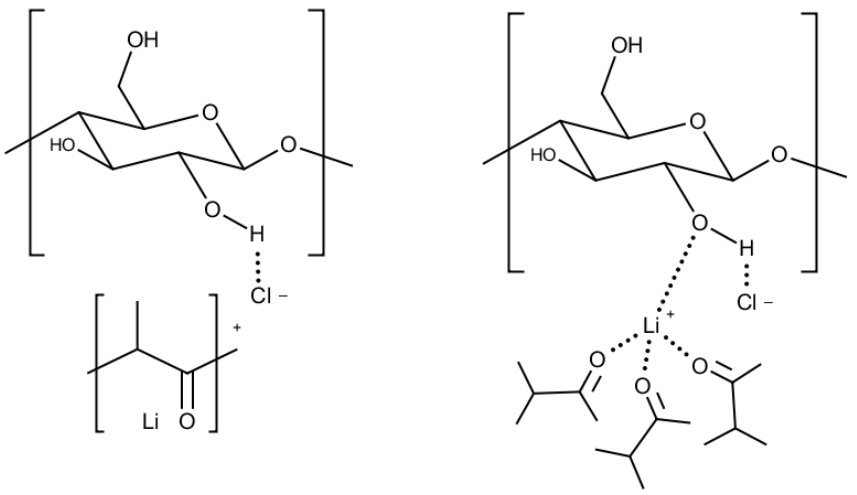

Figure 1.7 Cellulose dissolution mechanism in DMAc/LiCl proposed by McCormic [35] *(left) and Morgenstern* [36] *(right).*

Different solvent-cellulose structures have been proposed [35]–[38]. Typical dissolution mechanisms of cellulose in DMAc/LiCl suggested the existence of

Li^+ cations in cellulose/DMAc/LiCl solutions (Figure 1.7). McCormick hypothesized that the Li^+ (DMAc) macrocation complex associates with the Cl^-, and there is no direct interaction between the Li^+ and oxygen atoms in cellulose in solutions. Morgenstern [36] observed that the ^7Li NMR chemical shift is a function of cellulose concentration, which confirmed close interactions between the Li^+ cations and cellulose chains. Authors suggested that one DMAc molecule in the inner coordination sphere of Li^+ is replaced by one cellulose hydroxyl group when dissolving cellulose in DMAc/LiCl. The chloride ions form hydrogen bonds with the cellulose hydroxyl groups destroying the intermolecular and intramolecular hydrogen bonding patterns of the cellulose polymer. The macrocation is also thought to have a weak interaction with the cellulose molecules, contributing 10% to the dipolar−dipolar interaction between cellulose and DMAc [39], [40].

Several different methods have been developed for the dissolution of cellulose in DMAc/LiCl. Among them, a solvent exchange procedure is generally employed to dissolve cellulose [35]. Regeneration of cellulose dissolved in the DMAc/LiCl solvent system can be exploited for a tailored shaping of cellulose, but insufficient recycling of the expensive solvent system still prevents large-scale application. In literature, there have been reported transparent films [41] and fibres [42] of regenerated cellulose previously dissolved in DMAc/LiCl solvent.

1.2.2. Compression moulding technique

Compression moulding is one of the original processing methods for manufacturing plastic parts developed at the very beginning of the plastics industry. Although it is also applicable to thermoplastics, compression moulding is commonly used in manufacturing thermoset plastic parts. The initial form of the material is usually a moulding powder or pellets, melted and poured into a mould. The mould is pressed and the material shaped into whatever shape desired (Figure 1.8).

There are two different types of compounds most frequently used in compression moulding: bulk moulding and sheet moulding. When the mould consists of flat plates, different materials can be moulded together into laminated sheets. An example of a laminate of that kind is plywood. In plywood, layers of wood are adhered to one another and impregnated by a thermoset such as urea-formaldehyde, which forms a network when heated [43]. Common examples of compression moulded manufacturing materials are: electrical parts, buttons, buckles, flatware, electronic device cases and appliance housing. These types of products could also be made from cellulose composites instead of plastics.

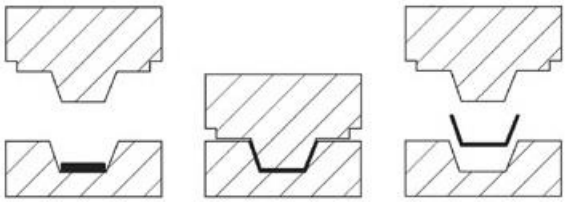

Figure 1.8 Simplified image of compression moulding process.

Compression moulding of cellulose pulp fibres under high pressure and elevated temperature provides an environmentally friendly process for preparation of stiff and strong cellulose materials. Cellulose can be processed into very high performance films and sheets. The first option uses solubilized cellulose fibres to produce very high performance sheets, similar to all-cellulose composite with a tensile strength of 480 MPa [44]. These amazing performances seemed to be possible only with the dissolution of cellulose using chemicals. The second option used repeated high pressure homogenizer treatments to reduce the size of the cellulose microfibrils to a nanometer scale. The suspension is concentrated with cold pressing, followed by an air drying step and a final hot pressing step. Compression moulding can be an alternative method to the time-consuming air drying process [45]. The group from Toulouse sussecfully compressed moulded pure α-cellulose into the dog bone specimens in short time with satisfacoty mechanical properties with a bending strength of 43.2 MPa, a bending modulus of 7.17 GPa, a tensile strength of 22.4 and a Young's modulus of 1.73 GPa [46]

1.2.3. Forging technique

Forging is a manufacturing process involving the shaping of usually metal using localized compressive forces. The blows are delivered with a hammer or a die. Forging is often classified according to the temperature at which it is performed: cold forging, warm forging, or hot forging. For the latter two, the metal is heated, usually in a forge. Forged parts can range in weight from less than a kilogram to hundreds of metric tons. Forging has been done by smiths for millennia. The traditional products were kitchenware, hardware, hand tools, edged weapons, cymbals, and jewellery. Since the Industrial Revolution, forged parts are widely used in mechanisms and machines wherever a component requires high strength; such forgings usually require further processing to achieve a finished part. Today, forging is a major worldwide industry.

Press forging works by slowly applying a continuous pressure or force, which differs from the near-instantaneous impact of hammer forging. The amount of time the dies are in contact with the workpiece is measured in seconds. The press forging operation can be done either cold or hot [47]. The main advantage of press forging, as compared to hammer forging, is its ability to deform the complete piece. Drop-hammer forging usually only deforms the surfaces of the metal piece in contact with the hammer and anvil; the interior of

the workpiece will stay relatively undeformed. Controlling the compression rate of the press forging operation, the internal strain can be controlled. There are a few disadvantages to this process, most stemming from the workpiece being in contact with the dies for such an extended period of time. The operation is a time-consuming process due to the number and length of steps. As the piece cools, it becomes stronger and less ductile, which may induce cracking if deformation continues. Therefore, heated dies are usually used to reduce heat loss, promote surface flow, and enable the production of finer details and closer tolerances. The piece may also need to be reheated.

When done in high productivity, press forging is more economical than hammer forging. Another advantage is that the operation can be used to create any size part because there is no limit to the size of the press forging machine. New press forging techniques have been able to create a higher degree of mechanical and orientation integrity. By the constraint of oxidation to the outer layers of the part, reduced levels of microcracking occur in the finished part. Press forging can be used to perform all types of forging, including open-die (Figure 1.9) and impression-die forging. Impression-die press forging usually requires less draft than drop forging and has better dimensional accuracy. Also, press forgings can often be done in one closing of the dies, allowing for easy automation.

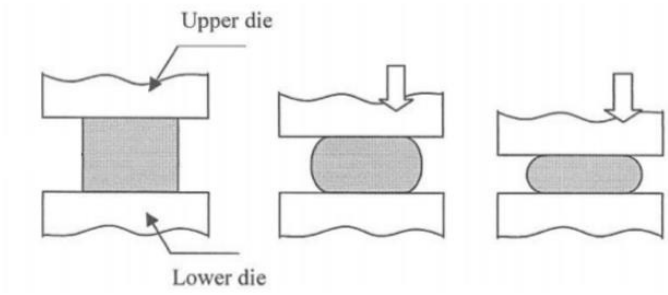

Figure 1.9 Simplified image of open-die forging process.

Apply high pressure (forging method) is one of the techniques that was studied extensively for metals and polyolefines. Pressure in the range of 200-400 MPa showed a change in the crystalline structure of polyethylene [48]. Most of the published studies of imposing high pressure on polysaccharides involve a combination of pressure and shear deformation at ambient temperature. Few studies explored possibilities of enhancing enzymatic hydrolysis after high-pressure treatment [49] or enhancing chemical reaction kinetics [50]. The effect of high pressure and temperature on dry and wet cotton linters was investigated [51], [52]. Results showed that wet samples had skin-core morphologies, where only the surface was destructured. Compressed dry cotton was fully

destructured, and the initial fibre structure was affected throughout the whole sample.

1.3. Bio-based composite

Composites are a combination of two materials. Generally, composites are prepared because the overall properties of the composite are better than the properties of individual components. A fibre reinforced polymer is a composite material consisting of a polymer matrix imbedded with high-strength fibres (Figure 1.10). Mainly, polymer matrix can be classified into two classes, thermoplastics and thermosetting. Thermoplastic materials currently dominate as matrices for natural fibre.

Figure 1.10 Image of a fibre reinforced composite.

A composite material comprising one or more phases derived from biological origin is bio-based composite. Natural fibres employed in bio-based composites include wood, flax, hemp, jute, sisal, kenaf, coir, kapok, banana, henequen and many others. The various advantages of natural fibres over man-made glass and carbon fibres are low cost, low density, comparable specific tensile properties, non-abrasive to the equipment, non-irritation to the skin, reduced energy consumption, lower health risk, renewability, recyclability and biodegradability [53].

There are many factors that can influence the performance of natural fibre reinforced composites. Apart from the hydrophilic nature of fibre, the properties of the natural fibre reinforced composites can also be influenced by fibre content. In general, high fibre content is required to achieve high performance of the composites. Therefore, the effect of fibre content on the properties of fibre reinforced composites is especially significant. It is often observed that the increase in fibre loading leads to an increase in mechanical properties of a composite [54], [55]. Naguib *et al*. [54] prepared bagasse fibres-polyester composite. Bagasse fibres were treated with 5% sodium hydroxide and then with dilute sulfuric acid. Bagasse–polyester composites were prepared by addition of 5, 10 and 15% of untreated and alkali treated bagasse fibres to polyester. The three point bending test indicated that an addition of treated bagasse filler to polyester matrix began to enhance both flexural strength and Young's modulus compared to untreated bagasse fibre.

Another important factor that remarkably influences the properties and interfacial characteristics of the composites is the processing parameters used. Therefore, suitable processing techniques and parameters must be carefully selected in order to yield the optimum composite products.

Natural fibres provide some challenges when used as a reinforcement phase in a polymer matrix. The mechanical properties of composite are influenced by the adhesion between the matrix polymer and its reinforcement phase [56], [57]. The major problem associated with untreated fibres and polymer matrix includes poor interfacial adhesion, limited thermal stability of the composite and poor fibre dispersion within the composite [58]. All plant derived cellulose fibres are polar and hydrophilic in nature. However, polyolefins such as polyethylene and polypropylene are nonpolar and hydrophobic materials. The incompatibility of the polar cellulose fibre and the non-polar matrix leads to poor adhesion, which then results in a composite with poor mechanical properties [59]. These challenges can be overcome with fibre treatment. The purpose of fibre treatment is to improve bonding between the fibre and the matrix. Fibre treatment can be physical, chemical or biological modification. Lu *et al.* [60] treated bamboo fibres with NaOH aqueous solution and silane coupling agent, respectively, before they were mixed with an epoxy resin. Compared with the untreated bamboo fibres filled epoxy composites, the NaOH solution treatment increased the tensile strength by 34% and elongation at break by 31%, while silane coupling agent treatment produced 71% enhancement in tensile strength and 53% increase in elongation at break.

Natural fibre-polymer composites are produced largely based on the existing techniques for processing plastics or composite materials. Some of the techniques include press moulding, extrusion, injection moulding, compression moulding and resin transfer moulding. Extrusion is a widely practiced processing method and a majority of the current composite materials based on thermoplastic polymers are processed by this method [61]. The lower thermal stability of natural fibres with up to 230 ºC, limits the number of thermoplastics to be considered as matrix material for composite manufacturing. Only those thermoplastics, whose processing temperature does not exceed 230 ºC might be considered for composites preparation. These are, most of all, polyolefines, like polyethylene and polypropylene. Technical thermoplastics, like polyamides, polyesters and polycarbonates require processing temperatures above 250 ºC, and therefore are not suitable for composite preparation without fibre degradation [62].

The main applications of bio-based composites are decking, consumer goods, car interior parts, house-wares, and construction [63]. Natural fibres can be used as substitutes for synthetic fibres in matrices, which show comparable characteristic values at lower costs. Moulded wood, natural fibre mouldings or laminated panels are generally used to make door panels.

1.3.1. Shellac resin

Shellac is derived from the secretion of a multitude of insects (e.g. *Laccifer lacca, Kerria lacca*) that are mostly cultivated in India and Thailand. It consists of a complex mixture of several polar and non-polar components [64]. The main acids, aleuritic acid and jalaric acid, are connected together by lactide and ester linkages, as illustrated in Figure 1.11. The hydrogen bonding network ensures the cohesion of the structure and gives the resinous character of shellac. Shellac can be fractioned into three main phases, namely hard resin (70%), soft resin (20-25%), and wax (5-10%). In its refined form, shellac is a polyester type of resin consisting of inter- and intra- esters of polyhydroxycarboxylic acids. The physical properties of the resin are an average molecular weight of 1006 Da, an acid value of 65-75 and a saponification value of 220-230.

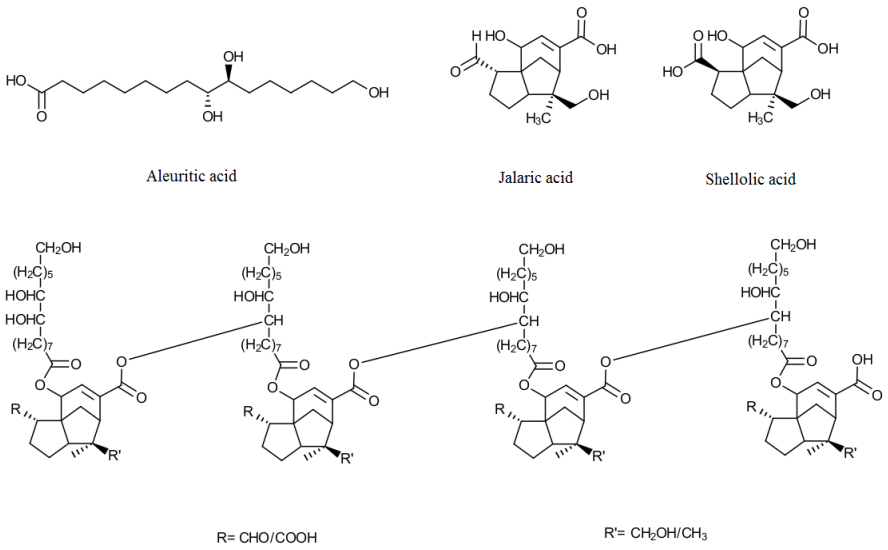

Figure 1.11 Chemical components and simplified structure of shellac resin [65][66].

Shellac is insoluble in water, hydrocarbon solvents and esters but dissolves readily in alcohol, alkali solutions, organic acids and ketones. In addition, dewaxed shellac melts from 75-80 ºC [67]. Shellac is made up of several fatty acids, partly in combination as inter-esters and partly free, and thus may be used for the same purpose as the vegetable oil. Edible shellac is used as a glazing agent on pills and sweets, in the form of pharmaceutical glaze. Because of its acidic properties, shellac-coated pills may be used for a timed enteric or colonic release [68]. Shellac is used as a coating on citrus fruit to prolong its shelf and storage life. It is also used to replace the natural wax of the apple, which is removed during the cleaning process [69]. When used for this purpose, it has the food additive number E904.

Shellac is traditionally used as a coating material. In fact, hydroxyl acids and polar groups present at the surface of the shellac molecule have the ability to orient themselves, which results in strong adhesion on many smooth surfaces. It provides glossy surfaces with good hardness and UV resistance. However, shellac films present a relatively low moisture and oxygen permeability. These properties are often discussed in view of food protection applications [70]–[72]. Furthermore, substantial literature reports can be found on the influence of additives and plasticizer (i.e. gelatin, starch and coconut oil) on film performance and processability [73]–[76]. In literature, there are relatively few papers on composite materials involving shellac. A few studies dealing with jute fibers and shellac are nevertheless interesting. In the first one, jute fibers were coated with shellac, so that fiber/matrix bonding at the interface was higher [77], while in the second one jute cloth was strengthened by impregnation with shellac [78]. Both studies show a good adhesion of shellac on natural fibers. However, there is a report of synthesized jute fiber reinforced aleuritic acid bio-based composites with supposedly good mechanical properties [79].

1.4. Bio-based foams

Polymer foams are found virtually everywhere in our modern society and are used in a wide variety of applications, such as disposable packaging, the cushioning of furniture and as insulation material. Polymer foams are made up of a solid and gas phase mixed together. The resulting foam has a polymer matrix with either air bubbles or air tunnels incorporated in it, which is known as either closed-cell or open-cell structure (Figure 1.12).

The gas that is used in the foam production is termed a blowing agent, and can be either chemical or physical. Chemical blowing agents are chemicals that take part in a reaction or decompose, giving off chemicals in the process. Physical blowing agents are gases that do not react chemically in the foaming process and are therefore inert to the polymer matrix.

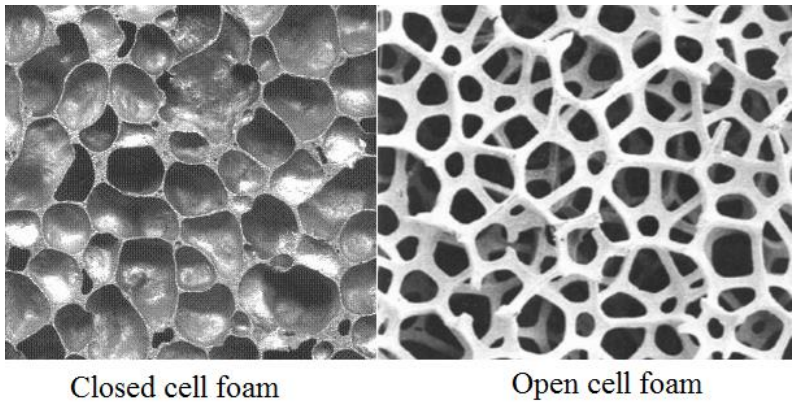

Figure 1.12 Image of open and closed cell foam [80].

Polymer foams are produced in a number of different ways, for instance by pouring, extrusion or different forms of moulding. Polymer foams can be divided into either thermoplastics or thermosets, which are further divided into rigid or flexible foams. The thermoplastics can usually be broken down and recycled, while thermosets are more difficult to recycle because they are usually heavily crosslinked [81].

Bio-based polymers have attracted considerable academic and industrial interest due to sustainability and environmental concerns. Therefore, the search for sustainable development based on renewable bio-based feedstocks has become a major research area. Biomass from plant-derived resources is renewable raw materials and is capable of providing a broad variety of starting materials of monomers and polymers that can be used in foam manufacturing. Bio-based foams are a fast growing industry, with a large contribution from plant-oil foams in the construction sector, and from starch foams in the packaging area.

Numerous natural fibres have been incorporated in foam systems, which generally provided a significant improvement in mechanical properties of the materials at appropriate fibre content. Composite foam has improved mechanical properties leading to satisfactory stress transfer in the composite system. It can be seen that the longer the fibres added into the system are, the stronger and stiffer the foams are. Moreover, with increasing fibre contents, the strain or flexibility of the composite foams decreases and the foam density increases [82].

Natural fibres have many benefits within foams derived from vegetable oil, beyond their advantages of renewability and potential biodegradability. Moisture content of natural fibres allows improved foaming kinetics and enhances interfacial interactions between fibres and foam matrix [83]. Moisture in natural fibres assists in the blowing process, where water is necessary, resulting in foams with slightly higher cell densities. For instance natural fibres cause noticeable improvement in mechanical properties compared to vegetable-oil-based foam without any reinforcement [84], [85]. Therefore, the incorporation of natural fibres holds potential towards improvements in a different set of foam properties.

Natural oils, which can be derived from both plant and animal sources, are plentiful in most parts of world. These oils are typically made up of triglycerides molecules. Triglycerides are composed of three fatty acids that vary in carbon length with 0 to 3 double bonds per fatty acid [86]. Triglycerides contain active sites amenable to chemical reaction. These active sites can be used to introduce functional groups on the triglycerides using the same techniques as applied in the synthesis of petrochemical polymers. Acrylated epoxidized soybean oil (AESO) can be synthesized from the reaction of acrylic acid with epoxidized soybean oil (Figure 1.13). Epoxidized soybean oil can be synthesized from soybean oil by common epoxidation reaction [87]. With the incorporation of acrylates, the soybean oil can react via additional polymerization.

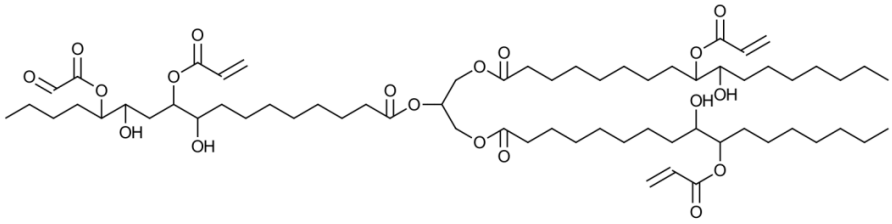

Figure 1.13 Molecular formula of acrylated epoxidized soybean oil.

Manufacturing of thermosetting foams from acrylated epoxidased soybean oil can be successfully done utilizing a pressurized carbon dioxide (CO_2) foaming process [88]. The foams' density can be controlled by the CO_2 pressure inside the reactor and by the vacuum applied during cure. Resulting foams had mechanical properties comparable with semi-rigid industrial foams.

Mechanical frothing is one of the most commonly used methods to create gas-liquid foams [89]. It is a mechanical process that creates gas inside the liquid phase from soybean-derived renewable monomer, which can be mixed with bacterial cellulose (BC) nanofibrils. Mechanically frothed gas-AESO-BC foam can be polymerised through microwave heating containing lauroyl peroxide as thermal initiator. The resulting macroporous polymer had a porosity of 60%, and foam stability was higher in case of bacterial nanofibrils presence. This was thought to be to the obstruction of the Plateau border in the presence of bacterial cellulose during capillary drainage of the monomer liquid. Bacterial cellulose contributed to higher mechanical properties as reinforcement. The incorporation of 0.5 wt% BC into the polymeric foams resulted in a significant increase of the specific Young's modulus when compared to the neat polymer foams. However, a further increase of BC to 1 wt% resulted in a decrease of the specific Young's modulus when compared to the neat polymeric foams.

Bio-based foam composite prepared using short sisal fibres as reinforcement and acrylated epoxidized soybean oil as matrix, can also be found in literature [90]. A study of the failure mechanism revealed that adhesion between fibre and matrix was a key issue responsible for damage of the foam, so interfacial interactions were enhanced with surface treatment of sisal fibres. Soil burial tests provided the information that the foams could be biodegradable. Compression tests demonstrated that sisal fibres are an effective reinforcement for AESO foams not only because the fibres have excellent mechanical performance but also because they are embedded in the foam matrix. AESO foam is characterized by strong and tough features with quite large compressive strain, and exhibit a comparable compressive stress to commercial polyurethane foam. Interfacial adhesion enhancement achieved by fibre pre-treatment by alkali or silane coupling agent leads to an improvement of foam performance.

2. Experimental

The pulp fibre raw materials that were used throughout the thesis were softwood dissolving pulp, pine pulp, and enoalfa dissolving pulp. Softwood dissolving pulp was provided by Domsjo Fabriker, Sweden (Cellulose 2100 plus). The pulp is produced from a controlled mixture of spruce and pine (60:40) by a two-stage sodium-based cooking to give a sulphite pulp with very low lignin content (0.6%) and high alpha-cellulose content (93%). The intrinsic viscosity of pulp was 530 ± 30 ml/g according to the ISO 5351 standard and the degree of polymerisation was 780 (Paper I and II). Pine pulp was acquired from Stora Enso Fabriker, Skutskär, Sweden. A pulp was produced from a controlled mixture of pine and spruce (70:30), and was used in Paper III. Enoalfa dissolving pulp, produced by Stora Enso Enocell pulp mill in Finland was used in foam preparation (Paper IV).

2.1. Chemical and mechanical treatment of pulp fibres

2.1.1. Swelling of pulp fibres in DMAc/LiCl solvent system

Cellulose material employed was softwood dissolving pulp, cut to small pieces. The cellulose was treated in the following ways: immersion in water followed by exchange to acetone and the further exchange to DMAc. Water was distilled from a tap in the laboratory. Reagent-grade acetone, DMAc, and LiCl were purchased from J.T Barker, Sigma-Aldrich and Merck respectively, and were used without further purification. The immersion in water acetone and DMAc was performed for one hour at ambient temperature. About 2 g of cellulose samples were immersed in 300 cm^3 of distilled water, 200 cm^3 of acetone, and 100 cm^3 DMAc. The specimens were vacuum-filtered after each solvent exchange.

After the above-mentioned activation procedure, cellulose samples were mixed with 50 cm^3 of DMAc and 3 g of LiCl, and the mixtures were allowed to stand at 40 ºC for 20 and 30 minutes. When the visible turbidity or solid residues were lost from the mixture, we regarded that the swelling of cellulose was completed. The illustration of the swelling process is presented in Figure 2.1.

When the swelling procedure was completed, a transparent gel was formed. The gel was solidified by distilled water and exchanged for fresh distilled water after 1, 4 and 12 hours. After solidification, the cellulose, referred to hereafter as Cell_DW, was dried at ambient temperature for further processing. A second solidification procedure involved the washing of a transparent gel with a solvent composed of isopropyl alcohol and deionized water (40:60). Samples were washed twice with 100 cm^3 of this solvent. After washing, the samples were soaked in 300 cm^3 deionized water to remove the residual isopropyl alcohol. Further, to remove the lithium from cellulose, samples were exposed to

running tap water overnight; the resultant product will be referred to hereafter as Cell_2PDW.

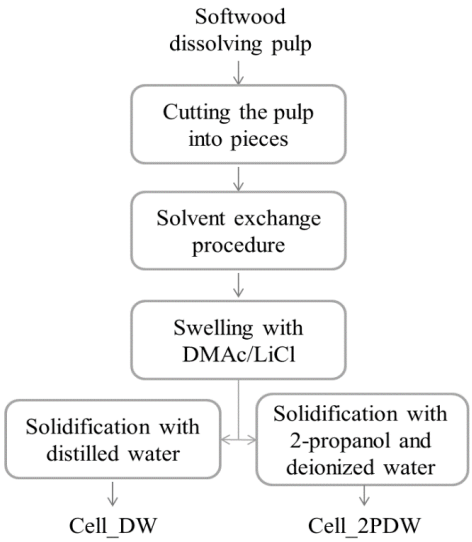

Figure 2.1 Flow chart presenting swelling process of pulp fibres in DMAc/LiCl solvent system.

2.1.2. 3D moulding technique

A cylindrical mould (Figure 2.2) with a piston was built of stainless steel. A dried sample was put in the mould, closed with the piston and placed on a regular hydraulic press (Enerpac bench press). Both samples (Cell_DW and Cell_2PDW) were pressed at approximately 70 MPa vertical pressure for a couple of seconds at ambient temperature.

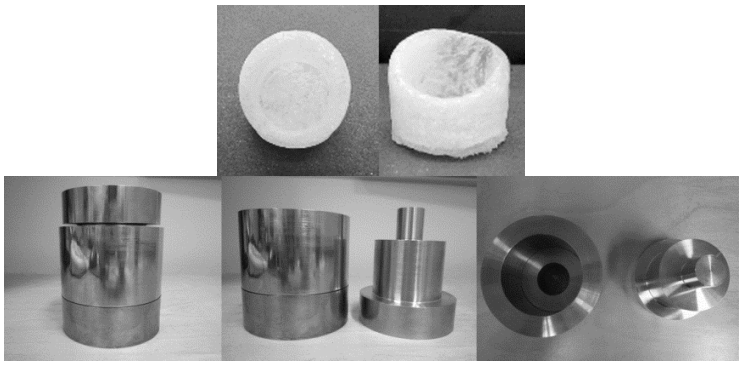

Figure 2.2 Image of moulded cellulose (up) and cylindrical prototype mould made of stainless steel (down).

2.1.3. Forging technique

The first medium pressure step was a precursor of the high pressure step. The cellulose sample Cell_DW or Cell_2PDW, weighting approximately 300 mg was placed on a cylindrical mould with a diameter of 10 mm. A cylinder, with two pistons, was made from 35 NiCrMo 16 steel. The cylindrical mould filled with the cellulose sample was placed in a hydraulic Carver press, as shown in Figure 2.3a. The pressure applied in the first step was 156 MPa (5 metric tons), during five minutes, producing cellulose cylinders. The cylinder thickness was 3 mm.

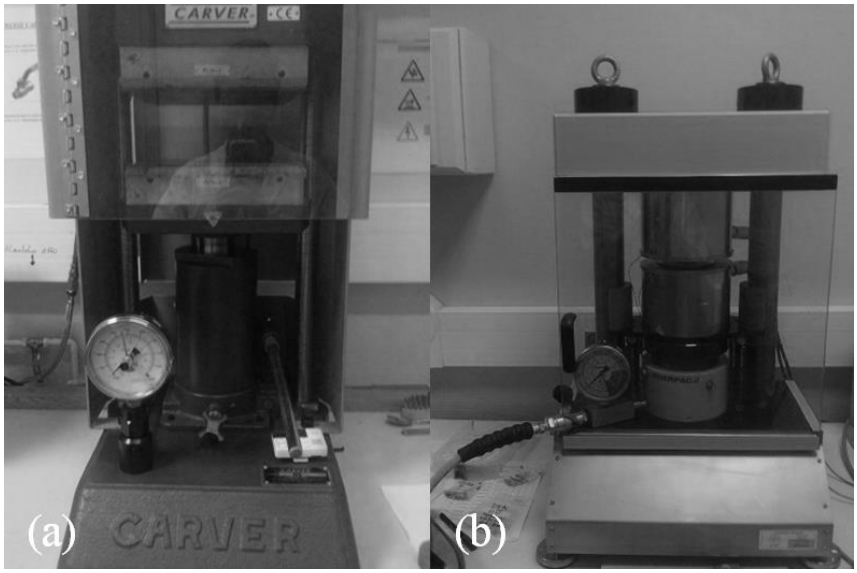

Figure 2.3 Image of Carver press (a) and Bridgman device (b).

The cellulose cylinders were placed in a cylindrical copper gasket ring. The first function of the copper rings is to confine the sample, preventing cellulose from escaping the pressure chamber. The second function of the copper rings is to provide an additional pressure as a result of its radial deformation during compression. To increase the deformability of the copper rings, a low dislocation density state was obtained by annealing the copper rings at 600 ºC for one hour. The Vickers hardness of the copper rings was measured as HV10=37. The cooper ring filled with cellulose was placed between the two anvils of the Bridgman device, showed in Figure 2.3b. In this home-made device, a cylinder is used to generate a compressive force applied with a foot hydraulic pump and measured pressure with a transducer. The cellulose samples were submitted to pressure between 0.5 and 0.9 GPa, during five minutes. Near 0.9 GPa applied pressure, the dislocation density of the copper ring was too high, causing the breaking of the ring under deformation. Pressure

above 0.9 GPa was not used. After compression, cellulose samples were a flat disk.

2.2. Bio-based composite preparation

2.2.1. Low consistency refining process

Pulp produced from a controlled mixture of pine and spruce (70:30) was refined. Low consistency (LC) refining of wood pulp was carried out at the laboratory refiner ProLab (Figure 2.4). Pine pulp was refined at energy of 200 kWh, in a refiner with disk fillings. Fibres flowed in grooves were collected by bar edges and transported into bar crossings where shear and compressive action takes place between opposing bar surfaces as mechanical energy is being transferred by forces. Pine pulp was physically refined in tap water. Water was then removed by filtering on Buchner funnel and, the pulp was washed with ethanol. Refined wood pulp was stored in excess of ethanol.

Figure 2.4 Image of low consistency refiner (ProLab).

2.2.2. Cellulose-shellac composite preparation

Refined pine pulp fibres and shellac resin in a ratio of 2:1 were vigorously mixed in composites preparation (Figure 2.5). The wax-free shellac was purchased from Fluka Analytical. To synthesize bio-based composite, different amounts of ethanol and polyethylene glycol (PEG) were added in a glass beaker and heated up to 135 ºC. Polyethylene glycol (DP ≈ 400) and ethanol (≥ 99.5%) were supplied from Sigma Aldrich. The melt mixture was poured into a tensile testing mould, and left for ten minutes. After the cooling period, the specimens were taken out of the mould.

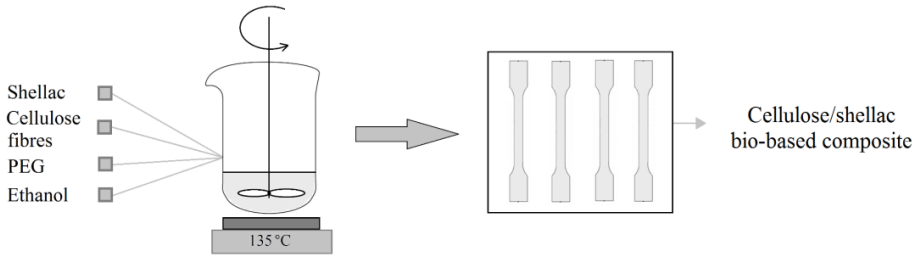

Figure 2.5 Flow chart of bio-based composite preparation.

The composition of the bio-based composite was 2:1=shellac:cellulose fibres. Since the cellulose fibres had different ethanol saturation, bio-based composite having 25% fibres and 75% ethanol will be referred to as She-Cell 25, the bio-based composite having 20% fibres and 80% ethanol will be referred to as She-Cell 20, and the bio-based composite having 15% fibres and 85% ethanol will be referred to as She-Cell15. Bio-based composite also contained polyethylene glycol in a ratio of 1:0.8= fibre: PEG.

2.3. Bio-based foam preparation

Enoalfa dissolving pulp was blended in a PolyMIX machine for 30 seconds, prior to foam formation. Polymer foams were prepared by thermally polymerizing the gas-fibre-AESO mixture (Figure 2.6). Acrylated epoxidized soybean oil was mixed with 1% t-butyl peroxybenzoate, 4% anionic surfactant ($CH_3(CH_2)_{11}SO_4Na$) and 5% blowing agent ($NaHCO_3$). Acrylated epoxidized soybean oil (Sigma-Aldrich), t-butyl peroxybenzoate (Sigma-Aldrich), Sodium hydrogen carbonate (Merck), and Sodium dodecyl sulfate (Sigma-Aldrich) were used as received without further purification.

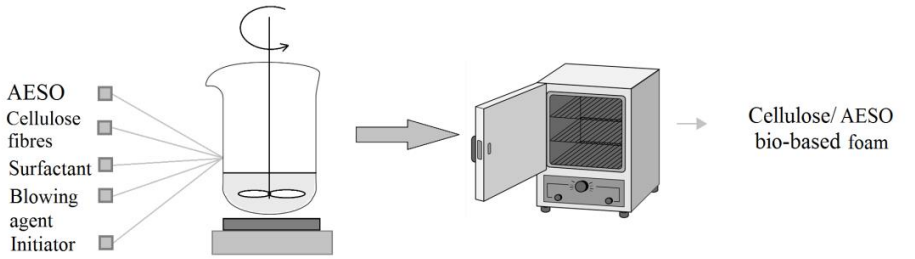

Figure 2.6 Flow chart of bio-based foam preparation.

The pulp fibres were introduced into the mixture in different weight fractions (2%, 3% and 4%). Addition of wood fibres increased the viscosity of mixture. A chemical blowing agent reacted when 0.5 ml of distilled water was added

into the system. The mixture was placed in an oven for 4 hours at 80 ºC. After polymerization, foams were left at ambient temperature to cool down for 24 hours. The post-curing procedure was performed at 110 ºC for 30 minutes.

2.4. Analytical methods

2.4.1. X-ray diffraction analysis (Paper I and II)

The XRD patterns of the softwood dissolving pulp, Cell_DW and Cell_2PDW (moulded and forged) were recorded at ambient conditions on an X-ray diffractometer (Bruker Discover D8, Germany). The specimens were mounted on glass discs with double-sided tape and measured. The intensity of radial scans for each sample was recorded using a Cu Kα radiation that was generated at an operating voltage of 40 kV and a filament current of 40 mA. The range of the scattering angle (2θ) was from 10 to 45º (scanning rate = 3 s/step, step size = 0.02º).

2.4.2. Raman spectrometry (Paper I)

Raman spectra of the softwood dissolving pulp, Cell_DW and Cell_2PDW were measured with the Thermo Scientific Nicolet iS50 spectrometer. The Raman system is equipped with a 1,064-nm diode laser. The laser power used for cellulose sample excitation was 500 mW, and 1,024 scans were accumulated. The softwood dissolving pulp was excited with 0.35 W power, and 32 scans were collected. The Omnic software programme was used to find peak positions and process the spectral data.

2.4.3. Inductively coupled plasma mass spectrometry (Paper I)

The softwood dissolving pulp, Cell_DW and Cell_2PDW were first digested with a microwave digestion system from Anton Paar (Multiwave 3,000). Sample amounts were balanced in a range of 0.1 g, and 5 cm^3 65% HNO3 from Merck and 1 cm^3 30% H_2O_2 were added. The temperature in the microwave oven was up to 200 ºC. The analysis was performed with an ICP-MS from Perkin-Elmer Sciex Elan 6100 DRC+. The standardisation was done with a multistandard from Ultra Scientific, item: IMS-102. The analysing method was the standard performance with the following parameters: sweeps: 11; replicates: 7; dwell time: 100; 10 ppb Rh was used as an internal standard solution.

2.4.4. Ultraviolet–visible spectrometry (Paper II)

The optical transmittance of the cellulose specimens Cell_DW and Cell_2PDW after high pressure treatment was measured from 200 to 1,000 nm, using a Shimadzu UV-Vis 2600 spectrometer equipped with an ICR-2600 Plus two-detector. The integrated sphere was coated with BaSO4. The UVProbe software program was used for analysing the data. Cellulose specimens with thicknesses

ranging from 0.2 mm to 2 mm were placed in a film holder and put inside the integrated sphere.

2.4.5. Attenuated total reflection infrared spectrometry (Paper III)

Bio-based cellulose-shellac composites were analysed by attenuated total reflectance (ATR) in the frequency range of 4,000 to 400 cm^{-1} on a Thermo Scientific Nicolet iS50 Spectrometer (Waltham, USA). A total of 64 scans were taken with a resolution of 4 cm^{-1}. The spectra were recorded in the transmission mode and converted into absorption for display. Omnic software (Thermo Scientific, USA) was used to find peak positions and process the spectral data.

2.4.6. Optical microscopy (Paper I)

The swelling mechanism of softwood dissolving pulp in the DMAc/LiCl solvent system was studied with a Nikon Eclipse E200 optic microscope attached to a Nikon DS-Fi2 digital camera. Swelling treatment was recorded after 10, 20 and 30 minutes.

2.4.7. Field emission scanning electron microscopy (Paper I, II, III and IV)

The morphology of Cell_DW and Cell_2PDW (moulded and forged), bio-based foam, and surface of a tensile fracture of bio-based composite was examined by a Leo Gemini 1530 field emission scanning electron microscope with an In-Lens detector (Germany). After moulding and high pressure treatment, samples were air-dried and sectioned using a doctor blade prior to being coated with carbon in a Temcarb TB500 sputter coater (Emscope Laboratories, UK). The cellulose-shellac composite and cellulose-AESO foam were also carbon coated. Optimum accelerating voltage was 2.70 kV.

2.4.8. 3D optical microscopy (Paper IV)

3D surface measurements of bio-based cellulose-AESO foams were examined by Bruker's 3D optical microscope system (Bruker Nano GmbH, Germany). Bruker Vision64 software provided functional and streamlined graphical user interface, and comprehensive data collection and analysis.

2.4.9. Tensile test (Paper III)

Mechanical properties of bio-based cellulose-shellac composite were measured with an Instron 8872 instrument (USA) using a force-controlled mode (10 mm/min). The sample had an average thickness of 0.45 cm, width of 0.45 cm and length of 3.20 cm. The average value of three to five replications was recorded. The calculated stress-strain curve revealed the following characteristic values: Young's modulus (E), yield strength, and maximal elongation.

2.4.10. Compression test (Paper IV)

Mechanical properties of bio-based cellulose-AESO foams were measured with an Instron 8872 instrument (USA) with a crosshead speed of 10 mm/min. The average value of five replications was recorded. The test specimens were cubes with a 10 mm long edge, except for the pristine AESO sample that were parallelepiped (10 x 10 x 5 mm). Bluehill 3 software provided data collection and analysis.

2.4.11. Nanoindentation test (Paper I, II, and IV)

Mechanical properties of moulded Cell_DW, Cell_2PDW (moulded and forged), and bio-based cellulose-AESO foam specimens were measured with UBI1 Nanomechanical Test Instrument (HYSITRON, Inc.) using a continuous stiffness measurement in a force controlled mode with a Berkovich type triangular diamond pyramid. Nanoindentation elastic modulus (E) and hardness (H) are defined from the following equations:

$$\mathrm{E} = \frac{1}{2}\frac{dP}{dh}\sqrt{\frac{\pi}{A}}$$

$$\mathrm{H} = \frac{Pmax}{A}$$

where P_{max} is the applied load at the maximum depth of penetration, A is the contact area and $\frac{dP}{dh}$ is the slope of the initial portion of the unload curve in the load-displacement plot. At least five indentations were performed on each sample, with a peak load force raging between 200 µN and 5,000 µN, and the average values were calculated. The nanoindentator was calibrated against different standards with a maximum standard deviation of 10%.

2.4.12. Contact angle analysis (Paper III)

Static contact angles of bio-based cellulose-shellac composites were measured with a KSV CAM 200 optical goniometer (KSV Instruments Ltd, Finland). The average value of five replications was recorded. A sessile droplet of 4 µL was placed on the composite surface, and the image of the drop was recorded over 60 seconds with a picture every 0.01 s during the first 5 seconds, and subsequently every 0.4 s. The static contact angle, defined by the intersection of the three-phase boundaries between liquid (l), solid (s), and vapour (v), was then determined by fitting the Young-Laplace equation around the droplet:

$$\gamma_{sv} = \gamma_{sl} + \gamma_{lv}\cos\theta$$

2.4.13. Argon pycnometer porosimetry (Paper IV)

Grain volumes of the cellulose-AESO foams were measured using an Ar pycnometer. The operation of pycnometer is based on applying the equation of state of ideal gas. The measurement set up consists of two chambers, pressure gauges and temperature gauges, an Ar-gas supply and a vacuum pump [91]. The bulk volumes of the bio-based specimens were determined by measuring dimension of them using a vernier caliper. The uncertainties of the measurements were determined using general law for propagation of uncertainty. Porosity (ε) can be defined using equation:

$$\epsilon = \frac{V_B - V_G}{V_B} \cdot 100\%$$

where V_B is the bulk volume and V_G the grain volume of the sample.

The grain-volume measurements results were averages over 10-12 independent measurements. The height of the sample was measured from several locations and their average was used when determining the bulk volumes. The given value for the pristine soy bean oil sample is highly uncertain due to the isolated pores that were not taken into account using pycnometry. When using an Ar-pycnometer the gas can only penetrate into pores that are connected to the surface and, thus, the given value overestimates the true grain volume and underestimates the porosity.

2.4.14. Thermal analysis (Paper IV)

The thermogravimetric analyses of the bio-based cellulose-AESO foams were carried out in a TGA–DTA thermoanalyser (Q Series instrument). Specimens of approximately 80-100 mg each were heated in corundum crucibles up to 500 ºC at a heating rate of 10 ºC per min in an argon atmosphere.

3. Results

3.1. Swelling of pulp fibres in DMAc/LiCl solvent system (Paper I)

Swelling is a process of increasing specimen volume via solvent absorption. The swelling process plays an important role in the chemical processing of cellulose. The purpose of a swelling step is usually to lower crystallinity and increase the accessibility of cellulose molecules. A solvent composed of N,N-methylacetamide and lithium chloride is suitable for characterization, processing, or homogeneous derivatization of cellulose. This solvent system can also be utilized as a swelling agent.

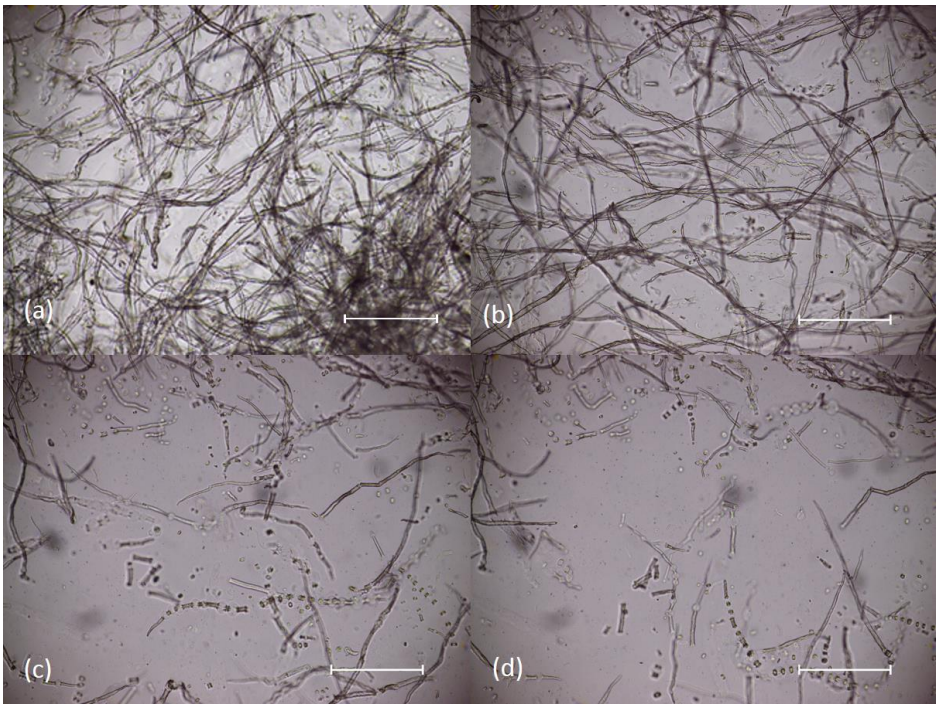

Figure 3.1 Optical images of softwood dissolving pulp fibres in DMAc/LiCl solvent system after (a) 5 minutes, (b) 10 minutes, (c) 20 minutes, and (d) 30 minutes. Bar represents 500 µm.

Swelling of cellulose fibres in the DMAc/LiCl solvent system is a heterogeneous process. The heterogeneous swelling of native cellulose fibres in the form of balloons scattered along the fibre was observed also in solvent systems like sodium hydroxide/water or a N – methylmorpholine N-oxide/water [92], [93]. When fibres are placed in DMAc/LiCl, solvent

molecules penetrate only to the selected parts of the fibre wall. The diffused molecules cause radial expansion of the secondary wall. These localised swollen parts along the fibre give the impression of balloons [94]. The balloons were formed in the first couple of minutes. In the course of swelling, the balloons were bursting and fragments arise. After 30 min of treatment, a two-phase system was visible (Figure 3.1) A few cellulose fibres seemed intact.

In the swelling process, Cl^- ions bond with the hydrogen atom of the hydroxide group (OH) of the cellulose molecule, and a new structure of hydrogen bonds is formed, breaking the existing bond network in the interior of the structure. Meanwhile, Li^+ ions interacted with the carbonyl group oxygen of the DMAc molecule, forming $[DMAc_nLi]^+$ macrocations. The original cellulose crystal network was destroyed enhancing solvation of macrocations on the cellulose macromolecule [95]. Macrocation stayed between cellulose chains preventing formation of intermolecular hydrogen bonds. When fibres swell, intermolecular bonds are broken as a result of the stress produced by the swelling process. Swelling of pulp fibres for 30 minutes was sufficient to reduce the crystallinity of cellulose to the necessary amount for the moulding process. A shorter swelling time would not decrease the crystallinity sufficiently, and would result in a brittle non-mouldable material.

Concentration of Li^+ ions in softwood dissolving pulp, Cell_DW and Cell_2PDW specimens is presented in Table 3.1. The Li^+ concentration of samples succeeding swelling in DMAc/LiCl was noticeably higher than compared with the reference soft dissolving pulp. The concentration of Li^+ ions reduced from 672 to 527 ppm decreased the swelling time from 30 to 20 minutes. An agreement can be reached that Li^+ ions stayed between cellulose chains, and the concentration of Li^+ ions was affected by the swelling time. Specimens solidified with 2-propanol and deionized water had observably lower amount of cations, indicating that solvent removed a larger part of the cations. This is in agreement with previously published findings [96]. A study showed an insignificant amount of DMAc and Li^+ ions (10.61 ppm) present in the films after washing with a 2-propanol and deionized water mixture, and subjecting it to running water. This solvent has much more power in dissociating cellulose with solvent complex than simple distilled water.

Table 3.1 Lithium ion concentration of softwood dissolving pulp (SWDP), Cell_DW and Cell_2PDW specimens.

Specimen	Content (mg/kg)	SD (mg/kg)	RSD (%)
SWDP	0.02	0.01	64.90
Cell_DW, 30 min	672.04	17.80	2.60
Cell_DW, 20 min	526.98	8.73	1.20
Cell_2PDW, 30 min	1.79	0.02	1.30

3.1.1. Effect of pulp fibres swelling on the cellulose structure

Information of the swollen cellulose structure was obtained from Raman spectra in the frequency region 300-3700 cm^{-1} (Figure 3.2). The Raman spectra for all samples display a highest peak located at 1095 cm^{-1}. It has been suggested that the peak located at 1095 cm^{-1} relates to the vibration of bonds within the backbone of the cellulose molecule and is dominated by the C-O stretching motion [97]. An alternative assignment to a stretching mode involving the glycosidic linkage (C–O–C) has also been suggested [7].

The broad band in the 3100-3600 cm^{-1} region that was due to the OH-stretching vibrations gave information regarding the hydrogen bonds. The peak characteristic of hydrogen bonds from the Cell_DW sample turned out to be wider compared to the peak from softwood dissolving pulp, which can be correlated with the interruption of the intra- and intermolecular hydrogen bond by swelling treatment. The Cell_DW spectrum exhibits a strong band at 605 cm^{-1} which is due to the bending motion of the O=C–N group of the DMAc molecule. Amide I band characteristic for C=O stretching vibration can be seen at 1650 cm^{-1}. This band is a typical carbonyl adsorption band of tertiary amides.

The Raman spectrum from sample Cell_2PDW was closer to softwood dissolving pulp spectrum, except for the lacking 605 cm^{-1} and 1650 cm^{-1} peaks. Generally, all amides have one or more bands of medium-to-strong intensity, which may be broad, in the region 695-550cm^{-1}, which are probably due to the bending motion of the O=C–N group. The carbonyl absorption band of tertiary amides occurs in the region 1670-1630 cm^{-1} [98]. The absence of these two peaks indicates the lack of DMAc molecules in Cell_2PDW samples. These findings are closely related and supported with mass spectroscopy data mentioned in section 3.1.

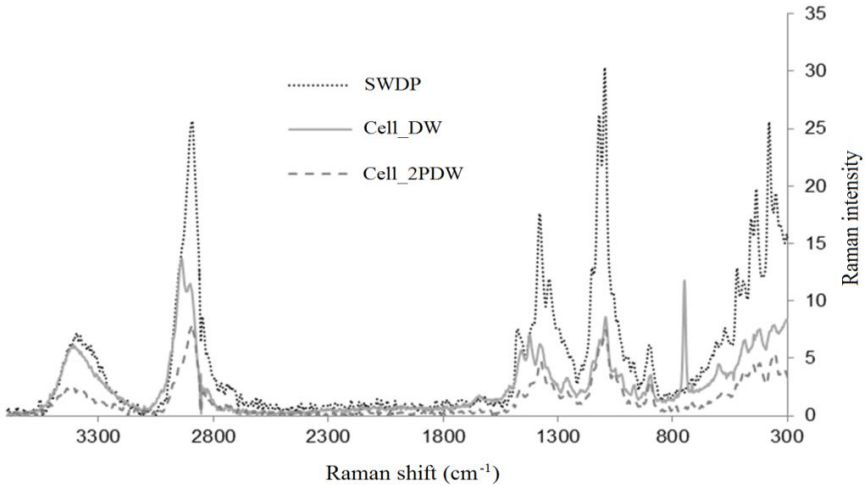

Figure 3.2 Raman spectra for softwood dissolving pulp, Cell_DW and Cell_2PDW specimens.

3.1.2. Effect of pulp fibres swelling on the cellulose crystallinity

Cellulose chains form an aggregate of highly ordered structures due to their chemical composition and spatial conformation. Cellulose exists in several crystal modifications, differing in unit cell dimensions and chain polarity. Native cellulose in wood has cellulose I crystalline modification with mainly a monoclinic unit cell. The physical properties and reactivity of cellulose is strongly influenced by the arrangement of cellulose molecules. Interactions between cellulose and reactive substances occur first in non-crystalline domains.

The X-ray patterns of softwood dissolving pulp, Cell_DW and Cell_2PDW are depicted in Figure 3.3. The x-ray diffractogram for the reference softwood dissolving pulp had two peaks, characteristic of the cellulose I crystal structure. The crystalline structure of cellulose was amorphous after swelling in DMAc/LiCl and solidifying with distilled water. A study of the transformation of microcrystalline cellulose, due to partial dissolution in 8% DMAc/LiCl, helped in understanding the phase transformation that occurs during dissolution in this particular solvent system. Dissolution occurs through the continuous peeling of layers of crystal domains. The peeled layers may retain some cellulose I structure from which they were removed, but generally they were too thin to contain crystallite chains. This is the reason why precipitated peeled layers seemed like amorphous cellulose [99].

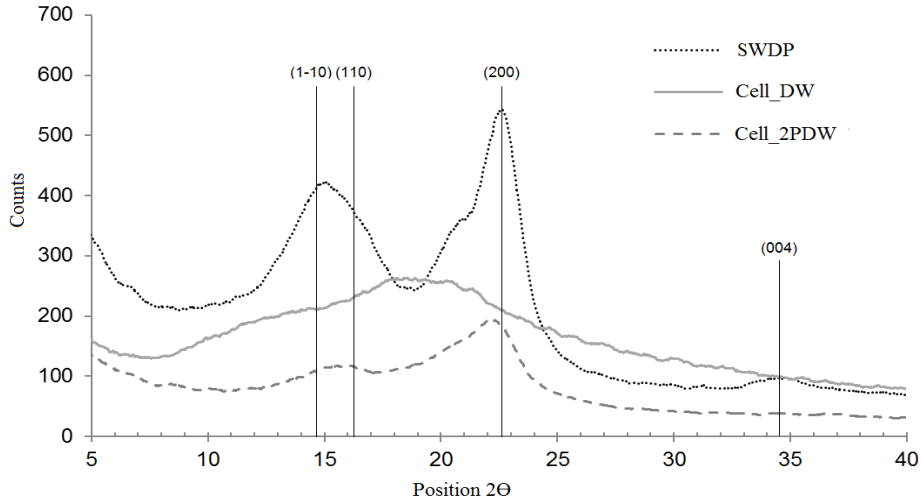

Figure 3.3 X-ray diffractogram of softwood dissolving pulp, Cell_DW and Cell_2PDW specimens.

Significant crystalline diffraction was not observed in Cell_DL specimens, indicating that the slow solidification of samples in distilled water produced crystallites of a small size or with imperfections in the crystalline structure. The Cell_RS specimen has diffraction peaks at 15.0° and 22.3°, indicating cellulose I structure.

3.2. 3D moulding and high pressure of swollen pulp fibres (Paper II)

3.2.1. Mechanical properties of chemimechanical treated pulp fibres

Nanoindentation technique was used to investigate the mechanical properties of the moulded and compressed specimens. The elastic modulus and hardness are shown in Table 3.2. For both types of cellulose specimens, the elastic modulus and hardness are relatively constant. The very weak trend to lower values observed at 0.9 GPa pressure was due to inhomogeneous deformation of the copper ring. Regarding the elastic modulus, there was a small effect of the applied pressure. The average value of the elastic modulus for system cellulose/distilled water was 2.9 GPa and for system cellulose/2-propanol/deionized water was 7.1 GPa. These values are in the range of the transverse modulus of cellulose fibres. Reported values for transverse modules for regenerated cellulose fibres have been between 4.9 and 6.7 GPa [100].

Table 3.2 Elastic modulus (Er) and hardness of Cell_DW and Cell_2PDW specimens after moulding, number specifies the value of high pressure.

Sample	Er (GPa)	Hardness (MPa)	Force (μN)	Depth (nm)
Cell_DW	0.05	6.5	200	3932
Cell_DW _0.5 GPa	2.8	140	500	974
Cell_DW_0.7 GPa	3.4	180	500	806
Cell_DW_0.9GPa	2.4	190	500	302
Cell_2PDW	7.0	380	5000	2839
Cell_2PDW_0.5 GPa	7.4	380	500	1100
Cell_2PDW_0.7 GPa	8.1	420	500	716
Cell_2PDW_0.9 GPa	5.7	300	500	607

The mean value of the hardness for cellulose regenerated with distilled water and regenerated with 2-propanol/deionized water was 170 MPa and 360 MPa, respectively. The increase of mechanical properties for both types of materials can be explained by higher compaction of material, leading to less free-volume areas between cellulose microfibrils. The values of mechanical properties were higher for the Cell_2PDW sample. This can be explained by the presence of cellulose crystalline phases which are transforming the material into a nanocomposite, with crystals reinforcing the non-crystalline phase. The strength of a starting material is a parameter controlling the mechanical properties of the compressed sample. In the case of compressed cotton, low strength fibres were easier to convert into many microfibers of nanometre size which are recombining into a compact material with better mechanical properties [51].

Compared to the mechanical properties of the moulded cellulose sample, a high increase of two orders of magnitudes for the elastic modulus and hardness was observed for cellulose compressed with high pressure. This can be due to several effects. The first is that the starting material had disordered structure with many tiny holes between cellulose fibrils oriented in different directions. Such a structure does not have a good mechanical resistance. Applying high pressure, fibrils are forced to move and fill holes, leading to much more compact structure, which in turn will show higher mechanical resistance. High pressure treatment decreases defects which are mainly voids, caused by trapped air bubbles in formed gel.

The second issue was difficulty to maintain the sample in the ring. Applying such high pressure led to matter escape which was probably changing an overall organisation. During medium and high pressure treatment, a small loss of material was noticeable. Pintiaux and coworkers [46] reported that dividing the initial mass by two led to a 63% increase of the Young's Modulus. Another effect of higher mechanical properties for a mentioned system can be in the chosen characterization method, since nanoindentation is probing a very thin layer located on the surface of a material. The sample surface which was directly in contact with anvils was more compact than the inner part of the material.

Lee *et al.* [101] investigated interphase properties in a cellulose fibre-reinforced polypropylene composite by nanoindentation. There was no significant difference among the mean value from 50 to 100 nm depth, and the unloading value at final indentation depth. The mean values for hardness and elastic modulus values were 0.62 and 16.62 GPa in the cellulose fibre and 0.11 and 3.03 GPa in the PP matrix, respectively. Gindl and Keckes [44] prepared an all-cellulose composite, in which both the fibres and the matrix are cellulose. The all-cellulose composite was prepared by distinguishing the solubility of the matrix cellulose into the solvent from that of the fibres via pretreatment. The tensile strength of uniaxially reinforced composite was 480 MPa, and the dynamic storage modulus was 20 GPa. These values were comparable to those of conventional glass-fibre composites.

3.2.2. Morphology of chemimechanical treated pulp fibres

The morphological structure of cellulose samples treated with DMAc/LiCl and moulded was observed via scanning electron microscopy images. The scanning electron micrographs (Figure 3.4 a) showed the heterogeneous and rough surface of moulded samples. Yun and co-workers [102] had similar findings. Curing of cellulose previously dissolved in DMAc/LiCl with deionised water led to objects with wrinkled rough surface and generated layered structure. FE-SEM images (Figure 3.4 b) display the microfibril bundles structure.

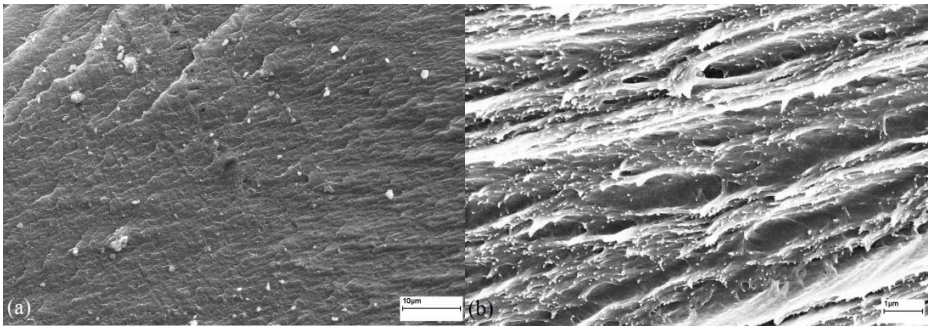

Figure 3.4 FE-SEM images of moulded cellulose surface (a), and moulded cellulose cross-section (b).

Wei and Cheng [103] studied the effect of solvent exchange on the structure of cellulose. They concluded that solvent activation of cellulose leads to the fibrillation of the treated fibre surface. These findings indicated that chemical and mechanical treatment of cellulose caused destruction of cell wall organisation and led to reorganisation of microfibrils into layers. Fibrils are destroyed by swelling treatment, and reassembled in a new structure.

FE-SEM observations of compressed samples are shown in Figure 3.5. The outer layer is highly compressed and had a different organization than the rest of the sample. The outer layer had a very good chain orientation which is giving linear propagation when detaching. This is suggesting that cellulose chains were oriented in the direction of the propagation.

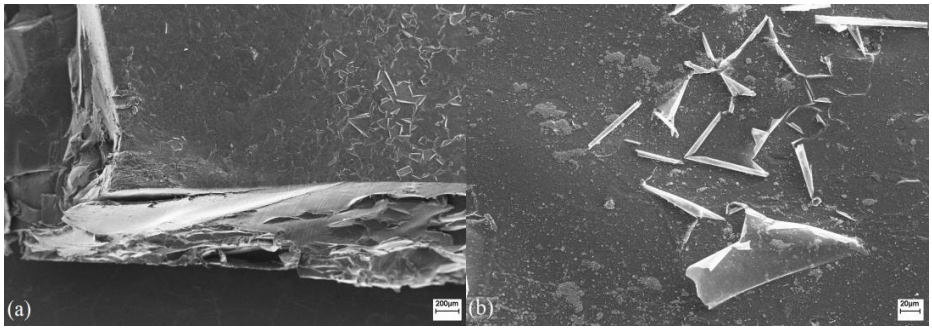

Figure 3.5 FE-SEM images of compressed cellulose sample viewed from the top (a), and compressed cellulose sample surface with rolled layers (b).

These thin surface layers were detaching by making very linear propagation as soon as the fracture initiation was made. There is no simple correlation between the fracture propagation angles, which is suggesting this layer was not monocrystalline. The thin peeled layer had a higher contraction at the outer surface than at the surface touching the sample, suggesting that the chains were oriented with an orientation factor decreasing from the surface to the inside of

the sample. The higher orientation of the outer layer is causing the rolling of many detached layers on surface. Diameters of rolls were between 5 and 12 μm, with an approximate thickness of the layer of 50-80 nm.

The inner part of a material had the different structure than the compacted surface. In most cases, the cross-section images of the compressed samples showed a layered structure with layers perpendicular to the compression plane. High compressed cellulose samples produced an inhomogeneous material composed of a compact rough surface and core with layered structure. High pressure treatment decreased surface defects which are mainly voids, caused by trapped air bubbles in formed gel.

3.2.3. Optical properties of compressed pulp fibres

The choice of anti-solvent in a solidification process had a great influence on the cellulose structure and its ability to interact with light. Addition of distilled water to the swollen cellulose mixture induced the formation of a purely amorphous sample, while addition of a mixture of isopropyl alcohol and deionized water produced cellulose samples with X-ray patterns typical of cellulose I crystals. Cellulose crystallinity has an impact on the overall transparency of materials formed either after addition of distilled water or 2-propanol and deionized water. Cellulose samples with crystalline regions had more opaque domains than the ones being non-crystalline, showing that crystallites are strongly scattering light. Therefore, crystallites must either be large or aggregated in such way that their dimension is close or larger than the wavelength of visible light. The difference of structure and its consequences on turbidity is kept when applying a pressure.

Figure 3.6 shows a clear difference between optical transmission spectra of the various cellulose samples. Submitted to such high pressures, samples are strongly compacting and no large holes were present, so the scattering from them is very low. The high transmittance difference between the two treatments is, thus, linked to the presence of crystalline scattering objects. The amorphous samples have a transmittance of about 70%. Its turbidity is due to a presence of small amounts of chromophores [104], which are absorbing light plus scattering linked to inhomogeneity in the organisation and orientations. Samples containing crystals have an average transmittance of around 30% in the visible range. The magnitude of applied pressure has an effect on the transmittance, with an increase of transmittance with increasing pressure. This effect, seen on both sets of samples, is explained with two factors, one being the further reduction of tine holes and the second the smaller thickness when pressure is increased.

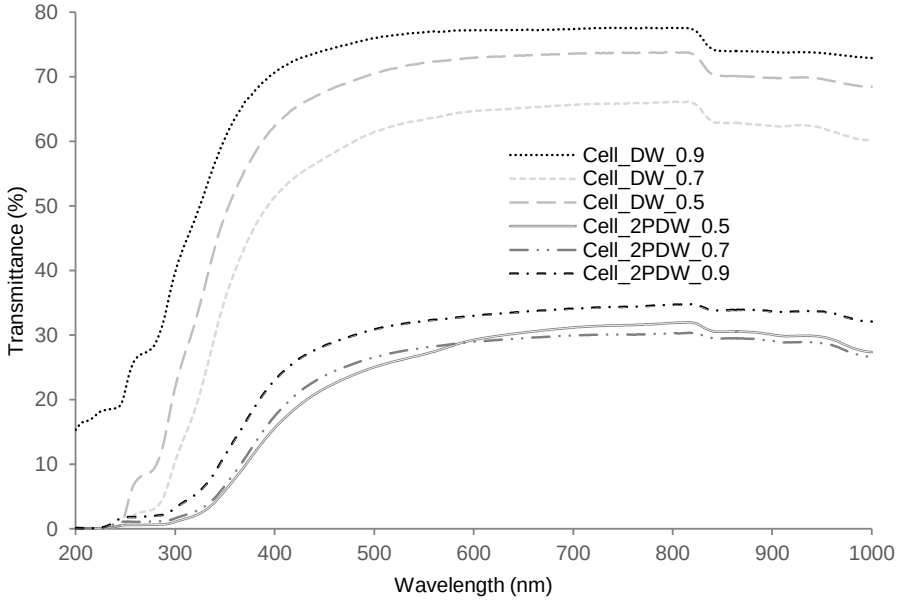

Figure 3.6 Optical transmission spectra for two types of swollen cellulose fibres pressed with high pressure. Cell_DW- samples washed with distilled water; Cell_2PDW- samples washed with a mixture of 2-propanol and deionized water; Numbers associated with each curve.

3.3. Bio-based cellulose-shellac composite (Paper III)

3.3.1. Structure of bio-based composite

Shellac has occupied the most important position among natural resins. It is not a single compound but rather consists of several polar and non-polar components. Shellac has been fractioned into three main components mostly hard resin, soft resin and wax. Both the resinous components of shellac contain hydroxyl acids. Shellac is readily dissolved in alcohol, organic acids and ketones but insoluble in water, hydrocarbon solvents and esters. This finding has led to believe that hydroxyl, carboxyl and carbonyl groups are present in shellac.

Shellac is a polyester type of resin consisting of polyhydroxy carboxylic acids. It is presumed to have five hydroxyl groups, one carboxyl group, three ester groups, one double bond and one aldehyde group in an average molecule. The chief building blocks of shellac are aleuritic acid and jalaric acid. Other isolated acids are butolic, shellolic, and laccialaric acids [67].

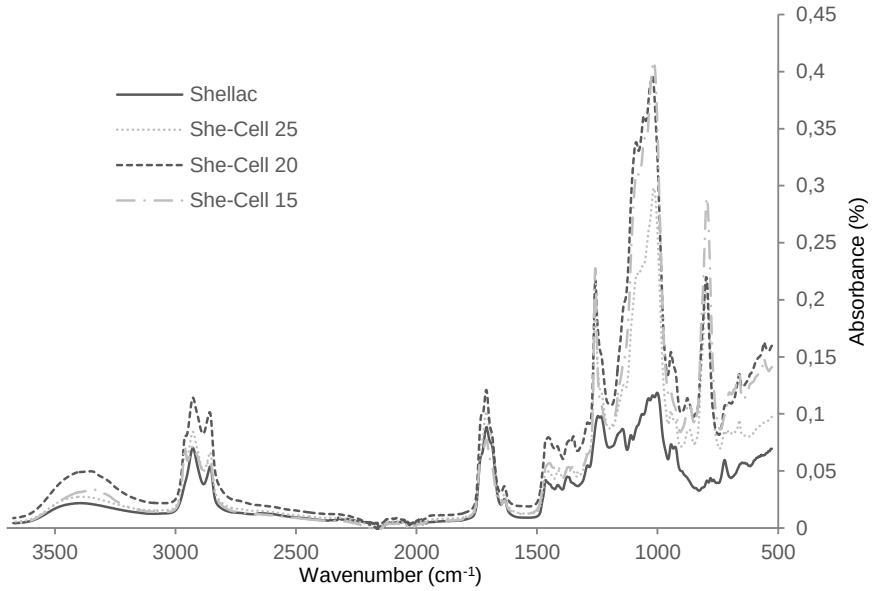

Figure 3.7 ATR spectra of shellac and bio-based She-Cell 25, She-Cell 20 and She-Cell 15 composite.

The ATR spectra of shellac and bio-based composite samples with different cellulose fibre amount are represented in Figure 3.7. The region between 1500 and 900 cm^{-1} is very characteristic for shellac. The spectrum was characterized by absorptions in the regions of 2923-2933 cm^{-1} and 2854-2858 cm^{-1} which are due to C-H stretching and 1464-1469 cm^{-1} and 1375-1377 cm^{-1} which result from C-H bending deformations. The spectra exhibit a broad absorption in the region of 3326-3421 cm^{-1} in the hydroxyl region [105]. The presence of cellulose is revealed by the absorption peak at 800 cm^{-1}, and the intensification of two groups of peaks at 1000, 1050, 1100, and 1750 cm^{-1}, that respectively correspond to the C-O stretch band of aliphatic primary, secondary alcohols and asymmetric ester [98]. There was no stronger absorption at 800 cm^{-1} and 1000 cm^{-1} peaks with higher cellulose content. Furthermore, the wide peak at 3400 cm^{-1} is slightly shifted to the left by increasing cellulose content, which is characteristic of the hydrogen bonds and interactions between cellulose chains, but also between the fibres and the matrix.

3.3.2. Mechanical properties of bio-based composite

Tensile strength is the maximum stress that a material can withstand while being stretched or pulled. Tensile strength is an important measure of a material's ability to perform in an application, and the measurement is widely used when describing the mechanical properties of materials.

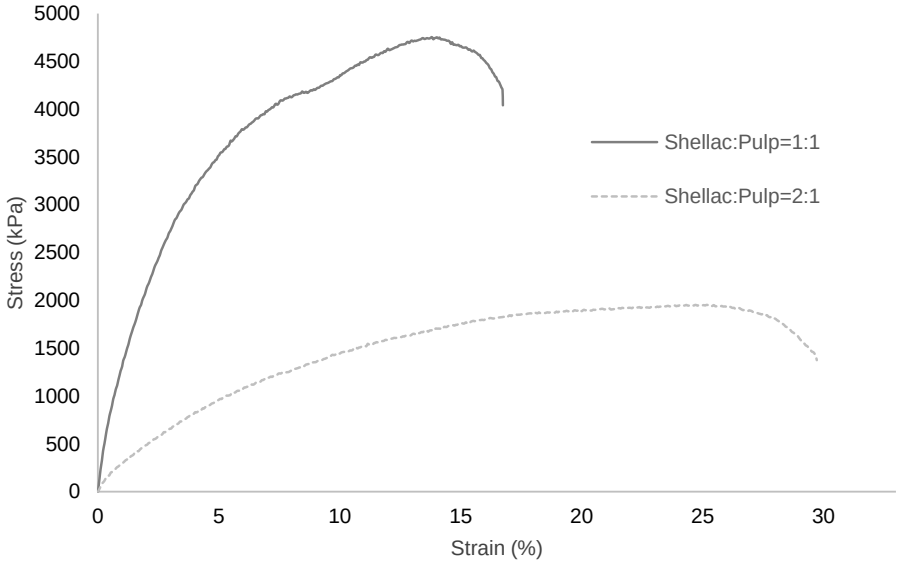

Figure 3.8 Stress-strain curves of bio-based composite regarding cellulose fibre and shellac ratio.

The bio-based composites with different ratios of matrix-reinforcement were synthesized and their mechanical properties are presented in Figure 3.8. The amount of cellulose fibres had an important impact on the mechanical performance. Young's modulus increased from 284 kPa to 1731 kPa, with increasing cellulose fibre amount in respect to shellac matrix. Generally the Young's modulus of the composite material increases with increasing fibre content [106]. Nevertheless, processing the material with high cellulose concentration was more difficult, and the composites obtained were anisotropic. Consequently, the maximal elongation was much lower.

The mechanical properties of bio-based composite with different fibre amounts are presented in Figure 3.9. The high value for elongation at break in the range of 30% to 35% was for bio-based composite She-Cell 15 and She-Cell 20. However, ethanol assisted in the dispersal of cellulose fibres into the matrix. At higher cellulose content, the breaking point often occurred earlier (20% of elongation) because of irregularities weakening the sample. In general, increasing the fibre content in the matrix led to a lower elongation at break of a composite [107]. In addition, as the fibre content increased, the shellac was insufficient to wet the fibre entirely and led to poor interfacial bonding between the fibre and the matrix. When force was applied, the composite had the tendency to fail rather than elongate. Unlike strain, the maximal stress depended on cellulose fibre content. For bio-based composite She-Cell 15 the maximal stress was less than 500 kPa, while it was around 2200 kPa and 1400 kPa for She-Cell 20 and She-Cell 25, respectively. Mechanical properties such as tensile strength and elongation at break of the raw shellac film were found to be 1.86 MPa and 4%, respectively [108].

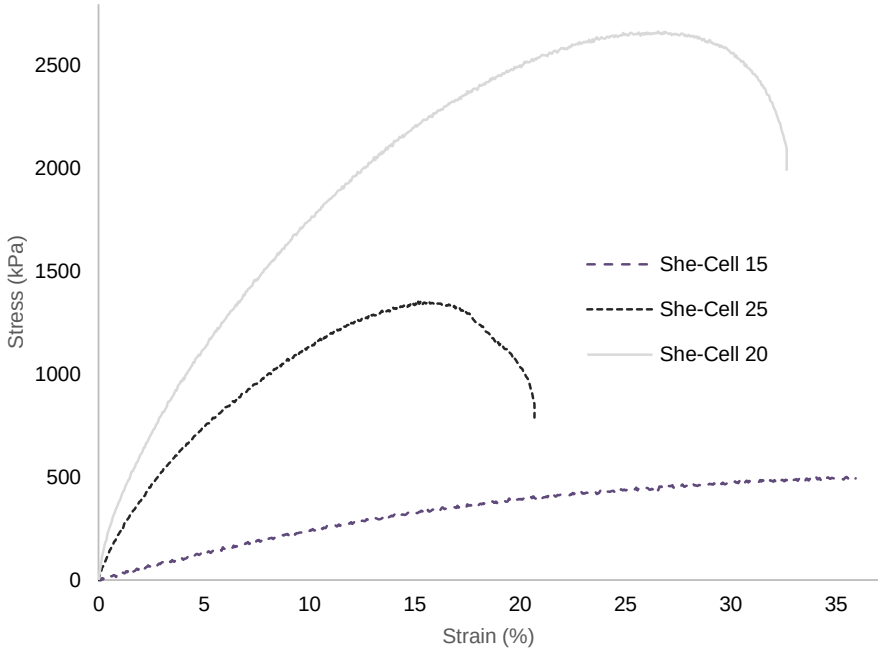

Figure 3.9 Stress-strain curves of bio-based composite.

Polyethylene glycol (PEG) in the function of a plasticizer was used to help the material process preparation. The mechanical properties of bio-based composite with different polyethylene glycol amounts are presented in Figure 3.10. When the concentration of PEG was higher the stress resistance was lower. The bio-based composites without plasticizer were more brittle and anisotropic. Shellac is composed of a hard resin that corresponds to a crystalline region formed through a chain-to-chain ester bond [74]. The structure of the crystalline structure generates the rigid and brittle characteristics of the shellac material. As a small molecular weight compound, PEG interfered with the shellac system, reducing the chain-to-chain ester bonds and, thus, increasing the composite flexibility. Additionally, polyethylene glycol was able to attract water which amplified the plasticizing effect.

When the PEG concentration increased, the stress resistance of the composite decreased. According to Qussi and Suess, addition of plasticizer caused a decrease in both the elastic modulus and glass transition temperature, and an increase in the elongation at break of free shellac films [109].

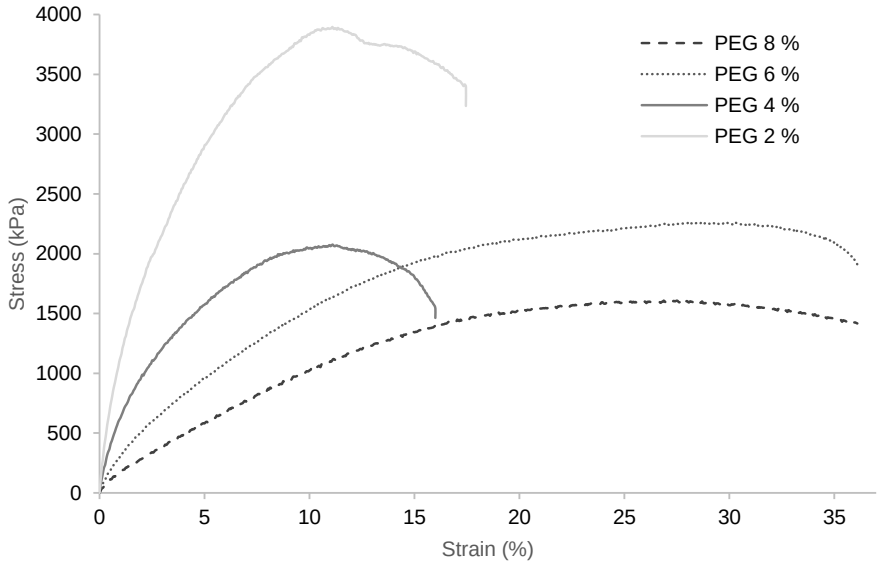

Figure 3.10 Stress-strain curves of bio-based composite regarding PEG content.

3.3.3. Contact angle of bio-based composite

The wetting phenomenon has received a huge interest from both fundamental and applied points of view. It plays an important role in many industrial processes, such as liquid coating, oil recovery, printing, lubrication, and spray quenching. In recent years, there has been an increasing interest in the study of superhydrophobic surfaces, due to their potential applications in, for example, nanofluidics, self-cleaning, and electrowetting [110]. Wettability studies usually involve the measurement of contact angles as the primary data, which indicates the degree of wetting when a solid and liquid interact. Small contact angles correspond to high wettability, while large contact angles correspond to low wettability.

Contact angles of bio-based cellulose reinforced shellac composite with different amount of fibre content is presented in Table 3.3. The contact angle increased slightly from 75° to 80° when the cellulose fibre content increased to 25% w/w. Contact angles lower than 90° indicated hydrophilic character and good wettability of the surface. The increase in wettability was in accordance with the higher total surface free energy, the lower dispersive force, and the higher polarity force with the increase in cellulose content. No adsorption was observed. Reported water contact angle of native shellac is 73° [111].

Table 3.3 Contact angle of bio-based composite with different cellulose fibre content.

Bio-based composite	She-Cell 15	She-Cell 20	She-Cell 25
Contac angle, º	75	80	80

3.3.4. Morphology of bio-based composite

Scanning electron microscopy (FE-SEM) analyses were evidence of the relation between the morphology and the mechanical behaviour of the bio-based composites. Composite She-Cell 25 had two visible phases (Fig. 3.11). Cellulose fibres were not dispersed uniformly in the matrix phase, but formed aggregates, while shellac formed a separate phase. Fibres, therefore, had no desired reinforcement effect on the matrix. As a result, the mechanical behaviour of the sample was close to pristine shellac.

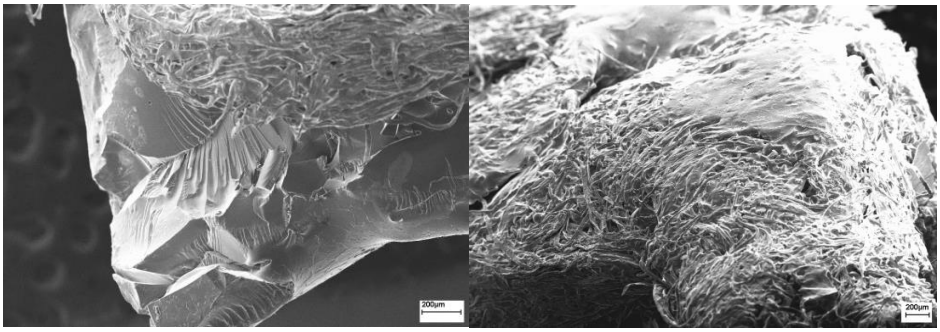

Figure 3.11 FE-SEM images of bio-based composite She-Cell 25.

Bio-based composite She-Cell 20 had much better dispersion of fibre reinforcement in the matrix phase (Figure 3.12). Shellac appeared to be softer and covered the fibres. This structure suggested more influence of fibres on the mechanical behaviour of the composite. In fact, at this level of cellulose dry content, the stress and the strain were higher than for She-Cell 25. However, holes that formed due to air bubbling during the curing process were observed. Improved properties could be reached with better curing conditions.

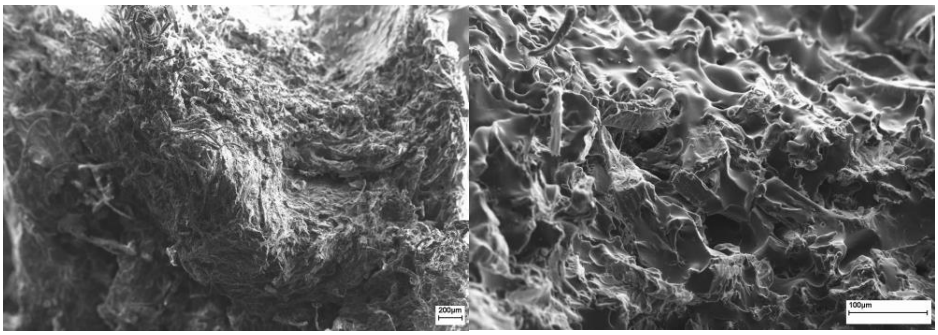

Figure 3.12 FE-SEM images of bio-based composite She-Cell 20.

Bio-based composite She-Cell 15 also had fibres well dispersed and coated by the matrix material. However, the stresses caused by mechanical testing broke

the matrix and pulled out the fibres (Figure 3.13). As a result, single fibres and voids appeared, demonstrating that lower amount of reinforcement led to lower stress resistance.

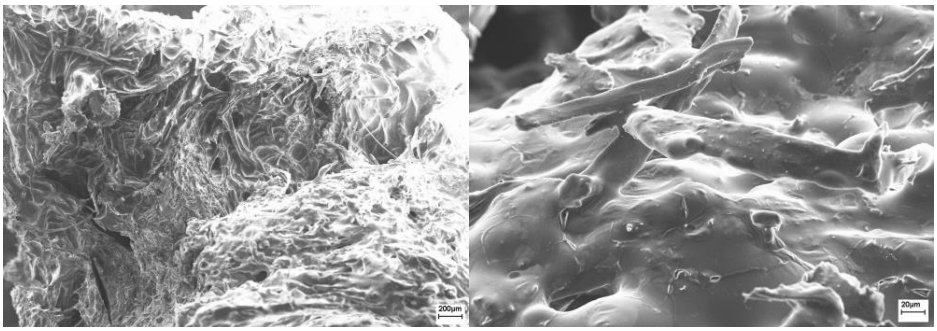

Figure 3.13 FE-SEM images of bio-based composite She-Cell 15.

3.4. Bio-based cellulose-AESO foam (Paper IV)

3.4.1. Porosity of bio-based foam

Porous materials are classified into several kinds by their pore size. Microporous materials have pore diameters of less than 2 nm, macroporous materials have pore diameters of greater than 50 nm, and the mesoporous category thus lies between 2 nm and 50 nm. No matter how big or small the space, it is called a void. The total amount of space inside a material is called porosity.

Porosity is one of the important parameters that govern the physical properties of porous materials. Porosity (ε) can be calculated with a measured grain and bulk volume of the material. One way to measure these volumes is using an Ar-gas pycnometer whose operation is based on applying the equation of state of ideal gas. Grain volume, bulk volume along with the porosity of bio-based foams are presented in Table 3.4.

Table 3.4 Grain volume, bulk volume and the porosity of bio-based foams.

	Grain volume V_G (cm^3)	**Bulk volume V_B (cm^3)**	**Porosity ε (%)**
AESO	1.58±0.05	1.65±0.06	4.5±4.4
AESO 2	1.92±0.05	4.45±0.15	57.0±1.8
AESO 3	2.16±0.05	5.17±0.15	58.3±1.5
AESO 4	2.08±0.05	4.55±0.15	54.2±1.8

From the results in Table 3.4, it is easily noticeable increase of the bio-based foam porosity from 4.5% to 57.0% with incorporating cellulose fibres. The introduction of cellulose fibres into the monomer phase resulted in stabilizing the gas-soybean oil interface during thermal polymerization, resulting in a rise of the total porosity. The highly porous nature of the bio-based foam AESO 3 is a direct result of the mixing process to introduce air bubbles into the bio-based soybean oil resin. Foam AESO 3 had the largest cell size compared to AESO 2 and AESO 4 foams.

The grain density and bulk density can be calculated from corresponding volumes and mass of porous material (Table 3.5). The density of solid polymeric foams typically range from 0.016 g/cm^3 to 0.960 g/cm^3, according to the requirements of a broad range of applications. High-density foams usually have a high mechanical strength and are used as lightweight structural components for furniture, transportation and construction. Medium-density foams are mostly used in packaging industry. Foams produced in this study are on the border between medium and high density materials. Requirements for structural applications are strong resistance to deformation and medium to high-density foams are preferred [112].

Table 3.5 Grain density and bulk density of AESO bio-based foam 2, 3, and 4 and AESO material.

	Grain density (g/cm^3)	**Bulk density (g/cm^3)**
AESO	1.55±0.04	1.48±0.04
AESO 2	1.28±0.02	0.538±0.004
AESO 3	1.134± 0.013	0.474±0.003
AESO 4	1.177±0.014	0.538±0.004

3.4.2. Morphology of bio-based foam

SEM images showing the internal structure and morphology of the pristine AESO material and cellulose reinforced AESO foams are shown in Fig. 3.14. Resulting images unveil randomly oriented pores with pore shapes that are semi-spherical and mostly highly irregular. Nevertheless, the pore size is highly non-uniform throughout the samples.

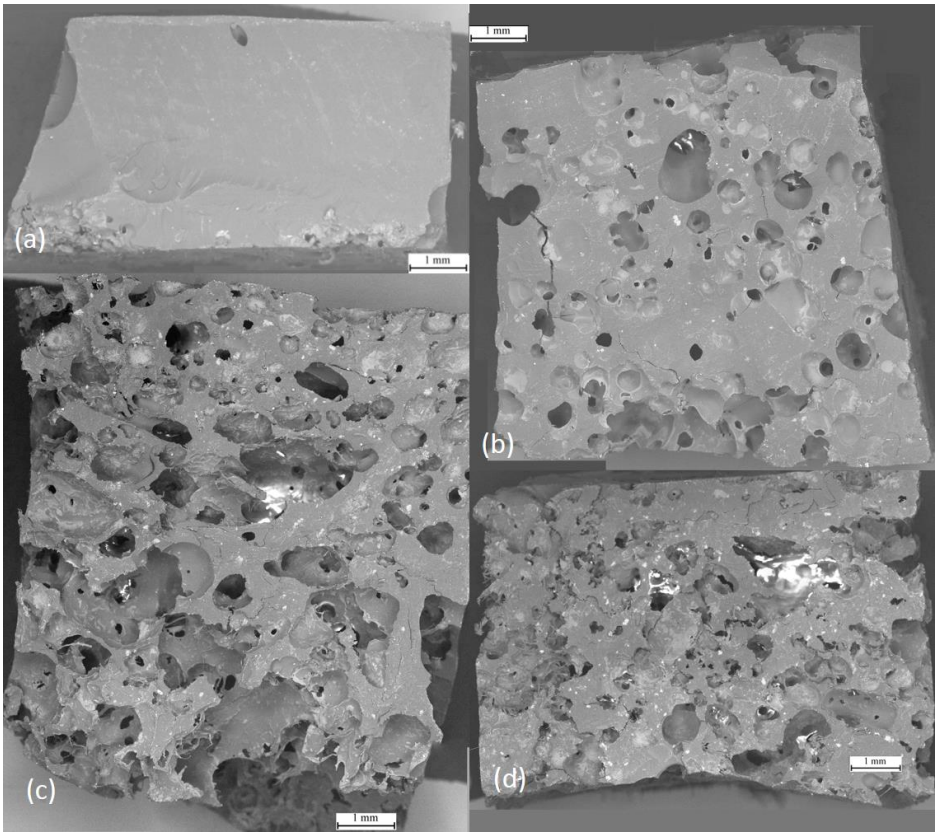

Figure 3.14 FE-SEM images of bio-based foams (a) AESO, (b) AESO 2, (c) AESO 3, and (d) AESO 4.

Foam is the dispersion of a gas in a liquid, which creates a characteristic structure when the matrix solidifies. Polymeric foams are usually prepared with liquid matrices, excluding expanded polystyrene closed-cell foams, made of pre-expanded polystyrene beads. The stability of a liquid matrix is governed by the dynamics of the thin interfacial films formed between air bubbles approaching each other. Two main reasons to foam destabilization are gravity and/or capillary drainage which induce film thinning and possible film rupturing unless prevented by repulsive electrostatic or steric forces between the film surfaces [113]. The foam which did not contain fibres, exhibited rapid destabilisation due to the expected fast kinetics of gravitational drainage, followed by capillary drainage, which ultimately resulted in the full phase separation of the foam. This phenomenon is clear in a case of pristine AESO foam presented in Figure 3.14 (a). This foam can be observed as solid material having a couple of closed-cell pores.

When the monomer phase contained fibres, the kinetics of destabilisation were significantly reduced (Figure 3.14 b, c, and d). Therefore, the porosity of

cellulose reinforced foams increased significantly. Incorporated fibres in the liquid phase will aggregate in the Plateau border, obstructing the flow of the liquid from the foam film [89].

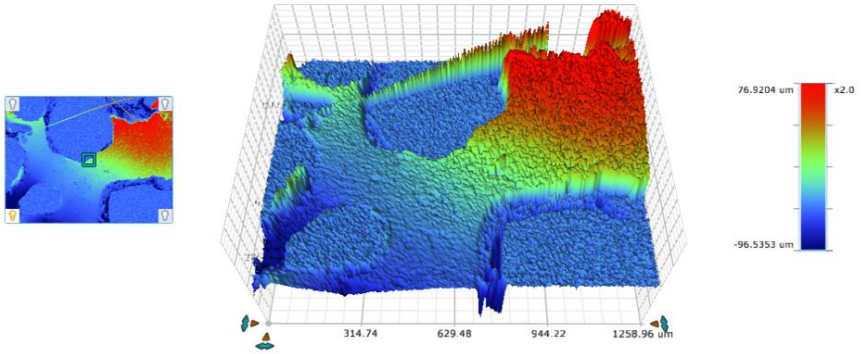

Label	Value	Units
Average	0.0022	nm
Data Points	307200	
Percent Data Points	100	%
Ra	15.89	µm
Rp	76.92	µm
Rq	21.80	µm
Rt	173.46	µm
Rv	-96.53	µm

Figure 3.15 The 3D image of AESO 2 bio-based foam with roughness information.

Addition of cellulose fibres resulted in an increase of cell size likely due to the increased number of nucleating sites induced by the fibre surfaces [114]. The cellulose reinforced foams had a less uniform pore structure, which should be related to the fibre distribution within the polymer matrix and the fibre-matrix interactions (Figure 3.15). With increasing cellulose fibres loading, the monomer phase became more viscous and the expansion of the gas bubbles in the monomer phase was hindered. This state of the bubbles results in the randomly orientated pores.

3.4.3. Mechanical properties of bio-based foam

Mechanical and physical properties of polymeric foams are related to the foam structure, which is controlled by the rates of bubble nucleation, bubble growth, foam aging and polymerization according to the laws of kinetics, thermodynamics and transport phenomena. The pores in the foam were formed by means of a chemical blowing agent followed by thermal polymerization of the liquid monomer. Acrylated epoxidized soybean oil is fascinating due to the high reactivity of the acrylic groups pertaining to easy polymerization via free radicals reaction.

Mechanical property, such as compressive strength of porous materials, is an important parameter that determines the application of foam. Compressive strength of AESO material and cellulose reinforced AESO foams is tabulate in Table 3.6. Results show that the compression strength of the cellulose reinforced foam increased with increasing fibre content, excluding pristine AESO material. Pristine AESO material had few closed-cell pores, so it was not considered as a porous material. When the foam cells are random and completely closed, the foams behave like solids, which correspond to a rise in compressive stress. Therefore, it is clear that neat AESO material had five times higher compressive strength compared to cellulose fibre foams.

This general model of an increase in strength can be attributed to the increased load-bearing capacity of the fibre reinforcements. Thus, the outcome compression strength indicated that introduction of fibres assisted in altering the response of the material during compressive loading. Increasing fibre amount in foams, the compressive strength of AESO foams slightly increased. The compressive yield strength of sawbones solid rigid polyurethane foam 30 pcf density is 18 MPa [115].

Table 3.6 Mechanical properties of AESO bio-based foam 2, 3, and 4 and AESO material.

	Maximum load (N)	**Yield strength (MPa)**	**Compressive strength (MPa)**
AESO	1498.0±157.6	28.4±3.3	29.9±3.1
AESO 2	351.2±11.5	3.7±0.2	4.7±0.1
AESO 3	558.5±11.0	4.3±0.2	5.5±0.1
AESO 4	589.9±16.7	4.0±0.2	5.9±0.1

Additional mechanical properties of the cellulose reinforced AESO foams and pristine AESO material were obtained by the nanoindentation method. Nanoindentation is widely used for the assessment of mechanical behaviour of the material microstructure. This method can provide useful information of the cell wall properties like hardness and reduced modulus. The values of the hardness and the reduced modulus of the cured AESO foams were determined from indentation curves. The overall behaviour of foam is directly dependent

on the formation of the individual phases and their microproperties. The nanoindentation tests were performed with a goal of increasing the knowledge of AESO foam microproperties.

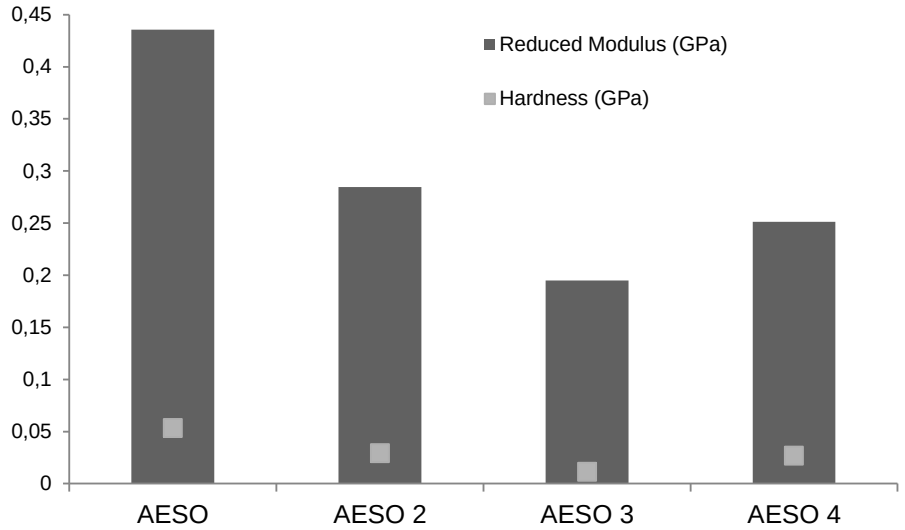

Figure 3.16 The hardness and reduced modulus of AESO bio-based foam 2, 3, and 4 and AESO material.

Nanoidentation results clearly show a difference in hardness and reduced modulus values for AESO material compared to AESO reinforced with cellulose fibres, as depicted in Figure 3.16. This distinction of mechanical properties can be explained with difference indenting compact material compared to probing porous material. Regarding the load-displacement curves for the cellulose reinforced AESO foams, all of them presented similar penetration depths and slopes, indicating that the AESO foam maintained its properties from the inner to the outer regions.

Porous materials show several types of heterogeneity at microscale. The heterogeneity originates from existing pores. The cellulose reinforced AESO foam had voids and material properties of the foam cell walls were affected by the indentation process. The overall behaviour of AESO foam is directly dependent on the formation of the individual pores and material micro-properties. With decreasing pore sizes and pore distances, the influence of the interphase material around the pore becomes more important and characteristic changes in the nano- and micro-deformation mechanisms appear [116]. Under load, structural openings, variations of local composition or orientation, nano-sized pores lower the mechanical properties of the material.

The effect of the cellulose fibre amount on mechanical properties can be described based on presented results. Initially, increasing the cellulose fibre amount from 2.0% to 3.0% decreased the hardness and reduced modulus of bio-based foam. Furthermore, increasing the cellulose fibre content from 3.0%

to 4.0% in the matrix increased the hardness and reduced the modulus values. Anyhow the obtained data were quite dependent on specimen surface. The inferior values of mechanical properties for AESO 3 foam can be connected to the highest porosity and pore size these foams had compared to the other two tested foams. The further rise of cellulose content indicated that the mechanical properties can be enhanced.

3.4.4. Thermal behaviour of bio-based foams

The thermal degradation behaviour of the pristine AESO material and cellulose reinforced AESO foams is depicted in Figure 3.17. Results show single-step degradation of all the tested samples in argon atmosphere. This single-step degradation originates from random polymer chain cleavage occurred during the heating of acrylated epoxidized soybean oil [117].

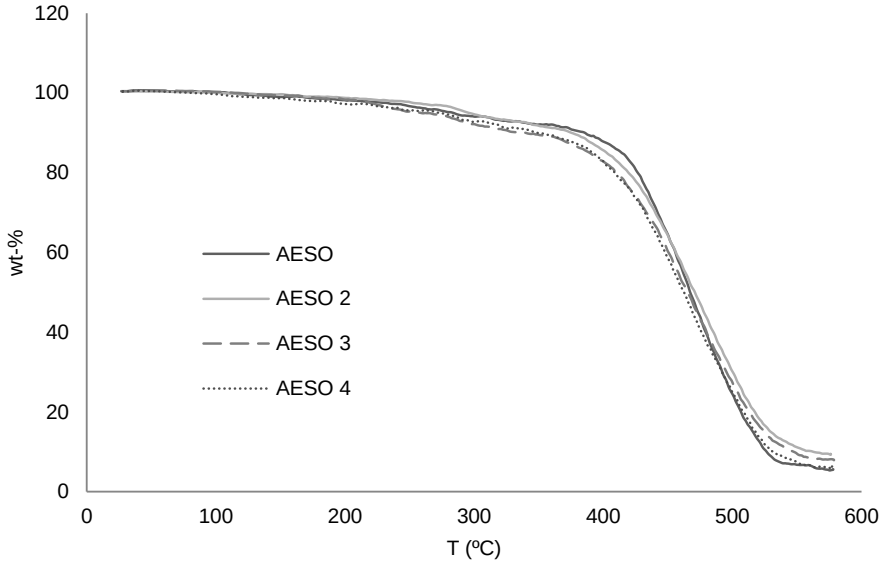

Figure 3.17 The thermal behaviour of AESO bio-based foam 2, 3, and 4 and AESO material.

The incorporation of cellulose fibres into the AESO matrix did not change the degradation behaviour of the final bio-based foam. This might be due to the low cellulose fibre content in the sample. The onset degradation temperature determined from TGA analysis of the foams was found to be 380 ºC for all samples. The residual carbon content was found to be slightly higher for the samples containing cellulose fibres compared to pure soybean oil polymer. The increase in the residual carbon content can be explained by the carbonisation of cellulose fibres in the mixture. TGA thermogram clearly indicates good thermal stability of the cured foams up to 300 ºC with a minimum amount of weight loss, which may be due to the minimum amount of unreacted components.

4. Concluding remarks

Currently, biomass is the largest and most important renewable resource used to produce different forms of materials and energy. Bioeconomy creates a demand for the use of more renewable feedstock in different applications. In the light of these demands this research was carried out. The goal of this work was a utilization of wood-base materials, with the accent on cellulose fraction for production of functional materials. This has been done by preparation of three different cellulose materials with different possible applications.

Cellulose swelling is essential for producing cellulose products. The DMAc/LiCl solvent system was used to swell cellulose, with the aim to take advantage of modifications in intermolecular chain interactions. The swelling process was necessary in breaking the existing bonds in the interior of the structure, and lowering crystallinity of the cellulose fibres. It can be accomplished using distilled water as an anti-solvent following the swelling reaction. Retained swelling solvent acted as a spacer between cellulose chains prohibiting formation of the hydrogen bonds. Separated cellulose chains had a disordered structure, which made them ductile and easily moulded. If solvent is washed away from specimens with anti-solvent, intermolecular hydrogen bonds are reformed. In that case, the material became brittle and lost its feasibility for moulding.

Preparation of bio-based composite materials composed of shellac in combination with different amounts of cellulose fibres and additives was carried out through a one-step procedure. Mechanically refined pine pulp fibres were used as reinforcements in manufacturing bio-based composite. The mechanical characterization of specimens showed that the reinforcement content and additive concentration had an impact on the mechanical properties. A wide range of samples with different properties was obtained, from hard material to soft.

Bio-based foams from cellulose fibres and an acrylated epoxidized resin were produced. The resin was mixed with different amounts of cellulose fibre, additives and thermally polymerized. The results show that it is possible to produce bio-based foams with satisfied mechanical properties without adding a reactive toxic comonomer like styrene. The stability of the gas-AESO interface was poor in comparison to the gas-AESO interface containing cellulose fibres. The incorporation of cellulose fibres into the polymeric foams exhibited increased mechanical properties. This was attributed to the reinforcing effect of the cellulose fibres. Thermal behaviour of macroporous polymer was not affected by the addition of cellulose fibres. FE-SEM images showed randomly oriented pores with irregular shapes and non-uniform pore size throughout the samples.

Mouldable cellulose material was dissolved prior to the moulding process, composite and foams are a mixture of green materials, produced according to very different processes. Mouldable cellulose had a unique mechanical

character and strongly depended on the kind of anti-solvent used in the manufacturing process. However, the production of composite and foams seems to depend entirely on the production process, and material formulation.

The widely used renewable materials are derived from wood and based on cellulose. However, major efforts are made to identify alternative uses of wood and agricultural resources. Materials derived from biomass can be used in the production of different types of materials using existing equipment and technology used for conventional materials. Nevertheless, these products have to be well performing in order to compete with highly developed currently used materials. It has been observed that lignocellulosic fibres are able to impart various benefits onto the polymer system. Therefore, cellulose fibres are interesting candidates due to the reinforcing effect they can bring to composite and foams.

5. Acknowledgments

The gratitude for my thesis goes to Professor Pedro Fardim for giving me the opportunity to be a part of his group after my graduation from the University of Belgrade. I am thankful for the chance to conduct my research in the fascinating area of biomass. I sincerely thank you for bringing the inspiration, and for sharing your knowledge and experience with me. I am deeply grateful for your willingness to help my professional development.

I am very grateful to Academic Lecturer Jan Gustafsson for the useful advice and unreserved support from the early stages of my research at FCT, and to Professor Patrick Navard for the expertise in material science and guidance during my scientific missions in France. Also, I would like to expand my gratitude to my colleagues from FCT, without whom I would not be where I am now. All my co-workers contributed one way or another to this dissertation.

I would like to thank all the co-authors in my publications from Åbo Akademi University, University of Turku, University of Helsinki, Centre de Mise en Forme des Materiaux in France, for their contribution to the successful collaboration.

Finnish Funding Agency for Innovation (Tekes), Graduate School of Chemical Engineering (GSCE), COST Action FP1205, and FinCEAL are gratefully acknowledged for valuable financial support.

I am a privileged person being surrounded by great family and good friends. I deeply appreciate their care and faith in me. I would like to thank all my friends for their support and encouragement through many years. Furthermore, my deep appreciation goes to my parents Radana Obradovic, Zivoslav Obradovic and my brother Igor Obradovic who supported me, especially during my quest for the doctoral degree. Special thanks go to my friend and colleague Aleksandra Vulicevic Davidovic, without whom I would not be in Finland.

Finally, I would like to express my deepest appreciation to my family, particularly to my husband Milos Arsic, my daughters Tara and Mila for being there for me. They were incredibly patient and surrounded me with plenty of love and wonderful moments. *Volim vas najvise!*

Jasmina Obradovic
Åbo, 2017

6. References

[1] C. Woodings, Woodings, and Calvin, "Fibers, Regenerated Cellulose," in *Kirk-Othmer Encyclopedia of Chemical Technology*, Hoboken, NJ, USA: John Wiley & Sons, Inc., 2003.

[2] L. K. J. Hauru, M. Hummel, K. Nieminen, A. Michud, and H. Sixta, "Cellulose regeneration and spinnability from ionic liquids," *Soft Matter*, vol. 12, no. 5, pp. 1487–1495, 2016.

[3] L. Shen, J. Haufe, and M. K. Patel, "Product overview and market projection of emerging bio-based plastics," *Gr. Sci. Technol. Soc.*, no. June, p. 41, 2009.

[4] L. Rebenfeld, "The Chemistry of Wood. B. L. Browning, Ed. Interscience (Wiley), New York, 1963. x + 689 pp. Illus. $25," *Science (80-.).*, vol. 142, no. 3599, p. 1564, 1963.

[5] H. F. J. Wenzl, *The Chemical Technology of Wood*. 1970.

[6] D. J. Cosgrove and M. C. Jarvis, "Comparative structure and biomechanics of plant primary and secondary cell walls.," *Front. Plant Sci.*, vol. 3, p. 204, 2012.

[7] N. Gierlinger, T. Keplinger, and M. Harrington, "Imaging of plant cell walls by confocal Raman microscopy," *Nat. Protoc.*, vol. 7, no. 9, pp. 1694–1708, Aug. 2012.

[8] W. G. Glasser, *Cellulose and Associated Heteropolysaccharides*. 2008.

[9] C. Laine, "Structures of hemicelluloses and pectins in wood and pulp," *Dep. Chem. Technol.*, vol. Doctor of, p. 63, 2005.

[10] N. S. Thompson, "Hemicellulose," in *Kirk-Othmer Encyclopedia of Chemical Technology*, John Wiley & Sons, Inc., 2000.

[11] R. Vanholme, B. Demedts, K. Morreel, J. Ralph, and W. Boerjan, "Lignin biosynthesis and structure.," *Plant Physiol.*, vol. 153, no. 3, pp. 895–905, 2010.

[12] C. Watt, "Improvement in the manufacture of paper from wood." Google Patents, 1854.

[13] M. A. X. Phillips, "Benjamin Chew Tilghman , and the Origin of the Sulfite Process for Delignification of Wood."

[14] J. Ward, *The perfection of the paper clip : curious tales of invention, accidental genius, and stationery obsession*. .

[15] C. J. Biermann, *Handbook of Pulping and Papermaking*, no. July. Academic Press, 1996.

[16] A. des sciences (France). A. du texte, "Comptes rendus hebdomadaires des séances de l'Académie des sciences / publiés... par MM. les secrétaires perpétuels," 1838.

[17] T. Liebert, "Cellulose Solvents – Remarkable History, Bright Future," *Cellul. Solvents Anal. Shap. Chem. Modif.*, pp. 3–54, 2010.

[18] A. F. Turbak, R. B. Hammer, R. E. Davies, and H. L. Hergert, "Cellulose solvents," *Chemtech*. p. 51, 1980.

[19] B. Philipp, B. Lukanoff, H. Schleicher, and W. Wagenknecht, "Homogene Umsetzung an Cellulose in organischen Lösemittelsystemen," *Zeitschrift für Chemie*, vol. 26, no. 2, pp. 50–58, Aug. 2010.

[20] T. Heinze and T. Liebert, "Unconventional methods in cellulose functionalization," *Prog. Polym. Sci.*, vol. 26, no. 9, pp. 1689–1762, 2001.

[21] C. Cuissinat, P. Navard, and T. Heinze, "Swelling and dissolution of cellulose. Part IV: Free floating cotton and wood fibres in ionic liquids," *Carbohydr. Polym.*, vol. 72, no. 4, pp. 590–596, 2008.

[22] I. V. M. Barbosa, D. M. Merquior, and F. C. Peixoto, "Continuous modelling and kinetic parameter estimation for cellulose nitration," *Chem. Eng. Sci.*, vol. 60, no. 19, pp. 5406–5413, Sep. 2005.

[23] A. A. Polyutov, Y. Y. Kleiner, V. M. Irklei, and L. S. Gal'braikh, "Study of the possibility of processing cotton cellulose in bulk for fabrication of viscose fibre," *Fibre Chem.*, vol. 32, no. 5, pp. 353–355, 2000.

[24] U. Ratanakamnuan, D. Atong, and D. Aht-Ong, “Cellulose esters from waste cotton fabric via conventional and microwave heating,” *Carbohydr. Polym.*, vol. 87, no. 1, pp. 84–94, Jan. 2012.

[25] S. C. Fox, B. Li, D. Xu, and K. J. Edgar, “Regioselective Esterification and Etherification of Cellulose: A Review,” *Biomacromolecules*, vol. 12, no. 6, pp. 1956–1972, Jun. 2011.

[26] M. W. Frey, “Electrospinning Cellulose and Cellulose Derivatives,” *Polym. Rev.*, vol. 48, no. 2, pp. 378–391, May 2008.

[27] C. Graenacher, “Cellulose solution,” 1934.

[28] T. Heinze and A. Koschella, “Solvents applied in the field of cellulose chemistry: a mini review,” *Polímeros*, vol. 15, no. 2, pp. 84–90, Jun. 2005.

[29] C. L. McCormick, “Novel cellulose solutions,” *U.S. Patent 4278790*. 1981.

[30] M. Strlič and J. Kolar, “Size exclusion chromatography of cellulose in LiCl/N,N-dimethylacetamide,” *J. Biochem. Biophys. Methods*, vol. 56, no. 1, pp. 265–279, 2003.

[31] A. El-Kafrawy, “Investigation of the cellulose/LiCl/dimethylacetamide and cellulose/LiCl/N-methyl-2-pyrrolidinone solutions by 13C NMR spectroscopy,” *J. Appl. Polym. Sci.*, vol. 27, no. 7, pp. 2435–2443, Jul. 1982.

[32] A. Synytsya and M. Novak, “Structural analysis of glucans,” *Ann. Transl. Med.*, vol. 2, no. 2, p. 17, Feb. 2014.

[33] T. Röder, B. Morgenstern, N. Schelosky, and O. Glatter, “Solutions of cellulose in N,N-dimethylacetamide/lithium chloride studied by light scattering methods,” *Polymer (Guildf).*, vol. 42, no. 16, pp. 6765–6773, 2001.

[34] E. Sjöholm, K. Gustafsson, B. Eriksson, W. Brown, and A. Colmsjö, “Aggregation of cellulose in lithium chloride/N,N-dimethylacetamide,” *Carbohydr. Polym.*, vol. 41, no. 2, pp. 153–161, 2000.

[35] C. L. MCCORMICK, P. A. CALLAIS, and B. H. J. HUTCHINSON, “Solution studies of cellulose in lithium chloride and N,N-dimethylacetamide,” *Macromolecules*, vol. 18, no. 12, pp. 2394–2401.

[36] B. Morgenstern, H. W. Kammer, W. Berger, and P. Skrabal, “7Li-NMR study on cellulose/LiCl/N.N-dimethylacetamide solutions,” *Acta Polym.*, vol. 43, no. 6, pp. 356–357, 1992.

[37] S. Spange, A. Reuter, E. Vilsmeier, T. Heinze, D. Keutel, and W. Linert, “Determination of empirical polarity parameters of the cellulose solventN,N-dimethylacetamide/LiCl by means of the solvatochromic technique,” *J. Polym. Sci. Part A Polym. Chem.*, vol. 36, no. 11, pp. 1945–1955, Aug. 1998.

[38] C. Zhang, R. Liu, J. Xiang, H. Kang, Z. Liu, and Y. Huang, “Dissolution Mechanism of Cellulose in N,N-Dimethylacetamide/Lithium Chloride: Revisiting through Molecular Interactions,” *J. Phys. Chem. B*, vol. 118, no. 31, pp. 9507–9514, 2014.

[39] A. M. Striegel, “Advances in the understanding of the dissolution mechanism of cellulose in DMAc/LiCl,” *J. Chil. Chem. Soc.*, vol. 48, no. 1, pp. 73–77, Mar. 2003.

[40] T. R. Dawsey and C. L. McCormick, “The lithium chloride/dimethylacetamide solvent for cellulose: A literature review,” *J. Macromol. Sci. Part C*, vol. 30, no. 3–4, pp. 405–440, 1990.

[41] B. Zhang, J. Azuma, and H. Uyama, “Preparation and characterization of a transparent amorphous cellulose film,” *RSC Adv.*, vol. 5, no. 4, pp. 2900–2907, 2015.

[42] Y.-K. Hong, K.-H. Chung, and W.-S. Lee, “Structure of Regenerated Cellulose Fibers from DMAc/LiCl Solution,” *Text. Res. J.*, vol. 68, no. 1, pp. 65–69, 1998.

[43] J. G. Drobny, *Handbook of Thermoplastic Elastomers*. Elsevier Science, 2007.

[44] T. Nishino, I. Matsuda, and K. Hirao, “All-Cellulose Composite,” *Macromolecules*, vol. 37, no. 20, pp. 7683–7687, 2004.

[45] H. Yano and S. Nakahara, “Bio-composites produced from plant microfiber bundles with a nanometer unit web-like network,” *J. Mater. Sci.*, vol. 39, no. 5, pp. 1635–1638, 2004.

[46] T. Pintiaux, D. Viet, V. Vandenbossche, L. Rigal, and A. Rouilly, “High pressure compression-molding of a-cellulose and effects of operating conditions,” *Materials (Basel).*, vol. 6, no. 6, pp. 2240–2261, 2013.

[47] E. P. Degarmo, J. T. Black, R. A. Kohser, and B. E. Klamecki, “Materials and process in manufacturing solutions manual.”

[48] M. Yasuniwa, M. Yamaguchi, A. Nakamura, and S. Tsubakihara, “Melting and Crystallization of Solution Crystallized Ultra-High Molecular Weight Polyethylene under High Pressure,” *Polym. J.*, vol. 22, no. 5, pp. 411–415, May 1990.

[49] S. C. T. Oliveira, A. B. Figueiredo, D. V. Evtuguin, and J. A. Saraiva, “High pressure treatment as a tool for engineering of enzymatic reactions in cellulosic fibres,” *Bioresour. Technol.*, vol. 107, pp. 530–534, Mar. 2012.

[50] S. Z. Rogovina, V. A. Zhorin, and N. S. Enikolopian, “Modification of cellulose in conditions of plastic flow under pressure,” *J. Appl. Polym. Sci.*, vol. 57, no. 4, pp. 439–447, 1995.

[51] E. Privas, E. Felder, and P. Navard, “Destructuration of cotton under elevated pressure,” *Cellulose*, vol. 20, no. 3, pp. 1001–1011, 2013.

[52] E. Privas, G. Gawrysiak, M. E. Lapeyre, M. Poitel, and P. Navard, “Influence of cotton variety on compression and destructuration abilities under elevated pressure,” *Cellulose*, vol. 20, no. 3, pp. 1013–1022, 2013.

[53] R. Malkapuram, V. Kumar, and Yuvraj Singh Negi, “Recent Development in Natural Fiber Reinforced Polypropylene Composites,” *J. Reinf. Plast. Compos.*, vol. 28, no. 10, pp. 1169–1189, May 2009.

[54] H. M. Naguib, U. F. Kandil, A. I. Hashem, and Y. M. Boghdadi, “Effect of fiber loading on the mechanical and physical properties of ‘green’ bagasse–polyester composite,” *J. Radiat. Res. Appl. Sci.*, vol. 8, no. 4, pp. 544–548, Oct. 2015.

[55] M. Das and D. Chakraborty, “Effects of alkalization and fiber loading on the mechanical properties and morphology of bamboo fiber composites. II. Resol matrix,” *J. Appl. Polym. Sci.*, vol. 112, no. 1, pp. 447–453, Apr. 2009.

[56] D. J. Gardner, G. S. Oporto, R. Mills, and M. A. S. Azizi Samir, “Adhesion and surface issues in cellulose and nanocellulose,” *J. Adhes. Sci. Technol.*, vol. 22, no. 5–6, pp. 545–567, 2008.

[57] J. M. Felix and P. Gatenholm, “The nature of adhesion in composites of modified cellulose fibers and polypropylene,” *J. Appl. Polym. Sci.*, vol. 42, no. 3, pp. 609–620, 1991.

[58] G. W. Beckermann and K. L. Pickering, “Engineering and evaluation of hemp fibre reinforced polypropylene composites: Fibre treatment and matrix modification,” *Compos. Part A Appl. Sci. Manuf.*, vol. 39, no. 6, pp. 979–988, Jun. 2008.

[59] N. P. G. Suardana, Y. Piao, and J. K. Lim, “Mechanical Properties of Hemp Fibers and Hemp / Pp Composites : Effects of Chemical Surface Treatment,” *Mater. Phys. Mech.*, vol. 11, pp. 1–8, 2011.

[60] T. Lu, M. Jiang, Z. Jiang, D. Hui, Z. Wang, and Z. Zhou, “Effect of surface modification of bamboo cellulose fibers on mechanical properties of cellulose/epoxy composites,” *Compos. Part B Eng.*, vol. 51, pp. 28–34, 2013.

[61] P. A. Fowler, J. M. Hughes, and R. M. Elias, “Review Biocomposites: technology, environmental credentials and market forces,” *J. Sci. Food Agric. J Sci Food Agric*, vol. 86, pp. 1781–1789, 2006.

[62] A. Bledzki, “Composites reinforced with cellulose based fibres,” *Prog. Polym. Sci.*, vol. 24, no. 2, pp. 221–274, May 1999.

[63] “Sustainable & Eco Friendly Sinks | Sloan.” [Online]. Available: https://www.sloan.com/commercial-bathroom-products/sinks/sustainable-bio-deck. [Accessed: 26-Jul-2017].

[64] B. B. Schaeffer and W. M. H. Gardner, “Nature and Constitution of Shellac,” *Ind. Eng. Chem.*, vol. 30, no. 3, pp. 333–336, 1938.

[65] “shellac composition.” [Online]. Available: http://ars.els-cdn.com/content/image/1-s2.0-S0264127515305475-gr1.jpg. [Accessed: 27-Sep-2017].

[66] “ExcshellacC001_default.png (430×258).” [Online]. Available: https://www.medicinescomplete.com/mc/excipients/2012/ExcshellacC001_default.png. [Accessed: 27-Sep-2017].

[67] S. K. Sharma, S. K. Shukla, and D. N. Vaid, “Shellac-Structure, Characteristics &

Modification," *Def Sci. J.*, vol. 33, no. 3, pp. 261–271, 1983.

[68] D. T. Mehring and S. S. Waukesha, "United States Patent," 1997.

[69] F. Standards, "Apples and Wax."

[70] R. D. Hagenmaier and P. E. Shaw, "Permeability of Shellac Coatings to Gases and Water Vapor," *J. Agric. Food Chem.*, vol. 39, no. 5, pp. 0–4, 1991.

[71] D. Phan The, F. Debeaufort, D. Luu, and A. Voilley, "Moisture barrier, wetting and mechanical properties of shellac/agar or shellac/cassava starch bilayer bio-membrane for food applications," *J. Memb. Sci.*, vol. 325, no. 1, pp. 277–283, Nov. 2008.

[72] O. P. Chauhan, P. S. Raju, A. Singh, and A. S. Bawa, "Shellac and aloe-gel-based surface coatings for maintaining keeping quality of apple slices," *Food Chem.*, vol. 126, no. 3, pp. 961–966, Jun. 2011.

[73] S. Soradech, S. Limatvapirat, and M. Luangtana-anan, "Stability enhancement of shellac by formation of composite film: Effect of gelatin and plasticizers," *J. Food Eng.*, vol. 116, no. 2, pp. 572–580, May 2013.

[74] P. Sittipaisankul, M. Luangtana-Anan, C. Limmatvapirat, and S. Limmatvapirat, "Enhanced Mechanical Properties of Shellac Films by Incorporation of Modified Coconut Oil," *Adv. Mater. Res.*, vol. 1060, pp. 119–123, Dec. 2014.

[75] Y. Byun, A. Ward, and S. Whiteside, "Formation and characterization of shellac-hydroxypropyl methylcellulose composite films," *Food Hydrocoll.*, vol. 27, no. 2, pp. 364–370, Jun. 2012.

[76] N. Poovarodom and W. Permyanwattana, "Development of starch/shellac-based composites for food contact applications," *J. Thermoplast. Compos. Mater.*, vol. 28, no. 5, pp. 597–609, May 2015.

[77] N. Shikamoto, P. Wongsriraksa, A. Ohtani, L. Y. Wei, and A. Nakai, "Processing and mechanical properties of biodegardable composites."

[78] M. Khan, S. Ghoshal, R. Khan, S. Pervin, and A. Mustafa, "Preparation and Characterization of Jute Fiber Reinforced Shellac Biocomposites : Effect of Additive," *Chem. Chem. Technol.*, vol. 2, no. 3, pp. 3–6, 2008.

[79] S. Biswas and B. C. Ray, "Preparation of Economically Viable and Environment Friendly Composites from Effluents of Aleuritic Acid Industry," *J. Polym. Environ.*, vol. 21, no. 4, pp. 1026–1031, Dec. 2013.

[80] "Open Vs. Closed Cell Foams | Foard Panel." [Online]. Available: http://www.foardpanel.com/open-vs-closed-cell-foams/. [Accessed: 27-Sep-2017].

[81] K. Sivertsen, "Polymer foams," *3.063 Polym. Phys.*, pp. 1–2, 2007.

[82] N. Soykeabkaew, C. Thanomsilp, and O. Suwantong, "A review: Starch-based composite foams," *Compos. Part A Appl. Sci. Manuf.*, vol. 78, pp. 246–263, 2015.

[83] L. M. Matuana and F. Mengeloglu, "Manufacture of rigid PVC/wood-flour composite foams using moisture contained in wood as foaming agent," *J. Vinyl Addit. Technol.*, vol. 8, no. 4, pp. 264–270, 2002.

[84] W. Liu, T. Xie, and R. Qiu, "Improvement of properties for biobased composites from modified soybean oil and hemp fibers: Dual role of diisocyanate," *Compos. Part A Appl. Sci. Manuf.*, vol. 90, pp. 278–285, 2016.

[85] M. Kuranska and A. Prociak, "Flax Fibers As Natural Filler for Rigid Polyurethane-Polyisocyanurate Foams Based on Bio-Polyol From Rapeseed Oil," *Tech. Trans. Chem.*, pp. 47–54, 2015.

[86] R. P. Wool and X. S. Sun, "Bio-Based Polymers and Composites," in *Bio-Based Polymers and Composites*, 2005, pp. 599–620.

[87] P. Number, "Process of epoxidation of oils," 1984.

[88] L. M. Bonnaillie and R. P. Wool, "Thermosetting foam with a high bio-based content from acrylated epoxidized soybean oil and carbon dioxide," *J. Appl. Polym. Sci.*, 2007.

[89] K.-Y. Lee, L. L. C. Wong, J. J. Blaker, J. M. Hodgkinson, and A. Bismarck, "Bio-based macroporous polymer nanocomposites made by mechanical frothing of acrylated epoxidised soybean oil," *Green Chem.*, vol. 13, no. 11, pp. 3117–23, 2011.

[90] S. P. Wu, J. F. Qiu, M. Z. Rong, M. Q. Zhang, and L. Y. Zhang, “Plant oil-based biofoam composites with balanced performance,” *Polym. Int.*, 2009.

[91] M. Voutilainen, M. Siitari-Kauppi, P. Sardini, A. Lindberg, and J. Timonen, “Pore-space characterization of an altered tonalite by X-ray computed microtomography and the14C-labeled-polymethylmethacrylate method,” *J. Geophys. Res. Solid Earth*, vol. 117, no. B1, p. n/a--n/a, 2012.

[92] N. Le Moigne and P. Navard, “Dissolution mechanisms of wood cellulose fibres in NaOH-water,” *Cellulose*, vol. 17, no. 1, pp. 31–45, 2010.

[93] B. Lindman, G. Karlström, and L. Stigsson, “On the mechanism of dissolution of cellulose,” *J. Mol. Liq.*, vol. 156, no. 1, pp. 76–81, 2010.

[94] P. Navard and C. Cuissinat, “Cellulose swelling and dissolution as a tool to study the fiber structure,” *7th Int. Symp. "Alternative Cellul. Manuf. Forming, Prop.*, p. 7 pages, 2006.

[95] H. Jing, Z. Liu, H. Y. Li, G. H. Wang, and J. W. Pu, “Solubility of wood-cellulose in LiCl/DMAC solvent system,” *For. Stud. China*, vol. 9, no. 3, pp. 217–220, 2007.

[96] J. N. Nayak, Y. Chen, and J. Kim, “Removal of impurities from cellulose films after their regeneration from cellulose dissolved in DMAc/LiCl solvent system,” *Ind. Eng. Chem. Res.*, vol. 47, no. 5, pp. 1702–1706, 2008.

[97] R. H. Atalla, *The structures of cellulose: Characterization of the Solid State*. American Chemical Society, 1987.

[98] G. Socrates, *Infrared and Raman characteristic group frequencies*. John Wiley & Sons, 2004.

[99] B. J.-C. Z. Duchemin, R. H. Newman, and M. P. Staiger, “Phase transformations in microcrystalline cellulose due to partial dissolution,” *Cellulose*, vol. 14, no. 4, pp. 311–320, 2007.

[100] W. Gindl *et al.*, “Anisotropy of the modulus of elasticity in regenerated cellulose fibres related to molecular orientation,” *Polymer (Guildf).*, vol. 49, no. 3, pp. 792–799, 2008.

[101] S.-H. Lee, S. Wang, G. M. Pharr, and H. Xu, “Evaluation of interphase properties in a cellulose fiber-reinforced polypropylene composite by nanoindentation and finite element analysis,” *Compos. Part A Appl. Sci. Manuf.*, vol. 38, no. 6, pp. 1517–1524, 2007.

[102] S. Yun, Y. Chen, J. N. Nayak, and J. Kim, “Effect of solvent mixture on properties and performance of electro-active paper made with regenerated cellulose,” *Sensors Actuators, B Chem.*, vol. 129, no. 2, pp. 652–658, 2008.

[103] Y. Wei and F. Cheng, “Effect of solvent exchange on the structure and rheological properties of cellulose in LiCl/DMAc,” *J. Appl. Polym. Sci.*, vol. 106, no. 6, pp. 3624–3630, 2007.

[104] A. Potthast, T. Rosenau, J. Sartori, H. Sixta, and P. Kosma, “Hydrolytic processes and condensation reactions in the cellulose solvent system N,N-dimethylacetamide/lithium chloride. Part 2: degradation of cellulose,” *Polymer (Guildf).*, vol. 44, no. 1, pp. 7–17, 2003.

[105] G. L. Shearer, “An Evaluation of Fourier Transform Infrared Spectroscopy for the Characterzation of Organic Compounds in Art and Archaeology,” no. October, pp. 1–399, 1989.

[106] H. Ku, H. Wang, N. Pattarachaiyakoop, and M. Trada, “A review on the tensile properties of natural fiber reinforced polymer composites,” *Compos. Part B Eng.*, vol. 42, no. 4, pp. 856–873, 2011.

[107] M. R. Ishak, Z. Leman, S. M. Sapuan, A. M. M. Edeerozey, and I. S. Othman, “Mechanical properties of kenaf bast and core fibre reinforced unsaturated polyester composites,” *IOP Conf. Ser. Mater. Sci. Eng.*, vol. 11, no. 1, p. 12006, 2010.

[108] S. Ghoshal, M. Khan, F. Gul-E-Noor, and R. Khan, “Gamma Radiation Induced Biodegradable Shellac Films Treated by Acrylic Monomer and Ethylene Glycol,” *J. Macromol. Sci. Part A*, vol. 46, no. 10, pp. 975–982, Oct. 2009.

[109] B. Qussi and W. G. Suess, “The Influence of Different Plasticizers and Polymers on the Mechanical and Thermal Properties, Porosity and Drug Permeability of Free Shellac Films,” *Drug Dev. Ind. Pharm.*, vol. 32, no. 4, pp. 403–412, 2006.

[110] Y. Yuan and T. R. Lee, “Contact Angle and Wetting Properties,” in *Surface Science Techniques*, G. Bracco and B. Holst, Eds. Berlin, Heidelberg: Springer Berlin Heidelberg,

2013, pp. 3–34.

[111] R. Lausecker, V. Badilita, U. Gleißner, and U. Wallrabe, “Introducing natural thermoplastic shellac to microfluidics: A green fabrication method for point-of-care devices.,” *Biomicrofluidics*, vol. 10, no. 4, p. 44101, Jul. 2016.

[112] L. M. Bonnaillie, “Bio-Based Polymeric Foam From Soybean Oil and Carbon Dioxide,” 2007.

[113] C. Monnereau, M. Vignes-Adler, and B. Kronberg, “Influence of gravity on foams,” *J. Chim. Phys. Physico-Chimie Biol.*, vol. 96, no. 6, pp. 958–967, Jun. 1999.

[114] A. Bergeret and J. C. Benezet, “Natural fibre-reinforced biofoams,” *Int. J. Polym. Sci.*, vol. 2011, pp. 1–14, 2011.

[115] MatWeb, “Solid Rigid Polyurethane Foam.” [Online]. Available: http://www.matweb.com/search/datasheet.aspx?matguid=09d08bbdc67040f894e7e17b51b70d7a&ckck=1. [Accessed: 27-Sep-2017].

[116] G. H. Michler and H.-H. K.-B. von Schmeling, “The physics and micro-mechanics of nano-voids and nano-particles in polymer combinations,” *Polymer (Guildf).*, vol. 54, no. 13, pp. 3131–3144, 2013.

[117] D. Behera and A. K. Banthia, “Synthesis, characterization, and kinetics study of thermal decomposition of epoxidized soybean oil acrylate,” *J. Appl. Polym. Sci.*, vol. 109, no. 4, pp. 2583–2590, 2008.

ISBN 978-952-12-3636-5